

Development of a Flexible Bridge Railing for Longitudinal Timber Decks

Submitted by

Ronald K. Faller, P.E.
Research Associate Engineer

Barry T. Rosson, Ph.D., P.E.
Associate Professor

MIDWEST ROADSIDE SAFETY FACILITY

Center for Infrastructure Research

Civil Engineering Department
University of Nebraska-Lincoln
1901 "Y" Street, Building "C"
Lincoln, Nebraska 68588-0601
(402) 472-6864

Submitted to

Michael A. Ritter, P.E.
Structural Engineer

FOREST PRODUCTS LABORATORY

U.S.D.A. - Forest Service
One Gifford Pinchot Dr.
Madison, Wisconsin 53705
(608) 231-9229

MwRSF Research Report No. TRP-03-62-96

June 1997

DISCLAIMER STATEMENT

The contents of this report reflect the views of the authors who are responsible for the facts and the accuracy of the data presented herein. The contents do not necessarily reflect the official views or policies of the United States Department of Agriculture, Forest Service, Forest Products Laboratory. This report does not constitute a standard, specification, or regulation.

ACKNOWLEDGMENTS

The authors would like to thank the following organizations who have contributed to the success of this research project: the American Institute of Timber Construction (AITC), Vancouver, WA, for donating the glulam materials used for the deck construction; and the Office of Sponsored Programs and the Center for Infrastructure Research, University of Nebraska-Lincoln, Lincoln, NE for matching support.

A special thanks is also given to the following individuals who made a contribution to the completion of this research project.

Midwest Roadside Safety Facility

Dean L. Sicking, Ph.D., P.E., MwRSF Director and Associate Professor
Brian G. Pfeifer, Ph.D., P.E., Research Associate Engineer
James C. Holloway, Research Associate Engineer
Kenneth L. Krenk, Field Operations Manager
Eric A. Keller, Computer Technician II
Douglas Whitehead, Former Civil Engineering Student
Undergraduate and Graduate Assistants

Dunlap Photography

James Dunlap, President and Owner

ABSTRACT

A low-cost, flexible W-beam bridge railing with "breakaway" posts was developed for use on longitudinal timber deck bridges located on low-volume roads. The bridge rail consisted of a 12-gauge (2.66-mm) W-beam rail supported by 3.5-in. by 5.5-in. (89-mm by 140-mm) dressed lumber posts spaced 6-ft 3-in. (1,905-mm) on center. Each post was placed between two 5-in. by 5-in. x $\frac{3}{8}$ -in. (127-mm x 127-mm x 9.5-mm) steel angles and connected to the vertical edge of the bridge deck with two $\frac{3}{4}$ -in. (19.0-mm) diameter by 12.0-in. (305-mm) long lag screws.

The research study included 37 static component tests, computer simulation modeling with BARRIER VII, and two full-scale vehicle crash tests using $\frac{3}{4}$ -ton pickup trucks. The first crash test, impacting at a speed of 31.2 mph (50.2 km/hr) and at an angle of 26.8 degrees, was unsuccessful because the vehicle vaulted over the bridge rail using a 24-in. (610-mm) top mounting height. Consequently, the height of the railing was increased to 27.78 in. (706 mm), resulting in a successful crash test at a speed of 30.6 mph (49.2 km/hr) and at an angle of 24.9 degrees. The safety performance of the bridge railing was determined to be acceptable according to the Test Level 1 (TL-1) evaluation criteria described in the National Cooperative Highway Research Report No. 350, *Recommended Procedures for the Safety Performance Evaluation of Highway Features*.

TABLE OF CONTENTS

	Page
DISCLAIMER STATEMENT	i
ACKNOWLEDGMENTS	ii
ABSTRACT	iii
TABLE OF CONTENTS	iv
List of Figures	vi
List of Tables	vii
1 INTRODUCTION	1
1.1 Problem Statement	1
1.2 Objective	1
1.3 Scope	2
2 LITERATURE REVIEW	3
2.1 Bridge Railings for Timber Deck Bridges	3
2.2 Other W-Beam Bridge Railings Systems	4
3 TEST REQUIREMENTS AND EVALUATION CRITERIA	5
3.1 Test Requirements	5
3.2 Evaluation Criteria	8
4 RAIL SYSTEM DEVELOPMENT - PHASE I	10
4.1 Design Considerations	10
4.2 Static Post Testing - Phase I	10
4.3 Design Details	15
4.3.1 Timber Deck and Substructure	15
4.3.2 Flexible W-Beam Bridge Railing System (Design No. 1)	15
4.4 Computer Simulation Modeling - Phase I	18
5 TEST CONDITIONS	20
5.1 Test Facility	20
5.2 Vehicle Tow and Guidance System	20
5.3 Test Vehicle	20
5.4 Data Acquisition Systems	23
5.4.1 Accelerometers	23
5.4.2 Rate Transducer	28
5.4.3 High-Speed Photography	29
5.4.4 Pressure Tape Switches	32

6 FULL-SCALE CRASH TEST - DESIGN NO. 1	33
6.1 TEST LVBR-1 (4,499 lbs (2,041 kg), 31.2 mph (50.2 km/hr), 26.8 degrees)	33
6.2 Test Description	33
6.3 Vehicle Damage	33
6.4 Barrier Damage	34
6.5 Occupant Risk Values	34
7 TEST LVBR-1 DISCUSSION	46
8 RAIL SYSTEM DEVELOPMENT - PHASE II	47
8.1 Static Post Testing - Phase II	47
8.2 Flexible W-Beam Bridge Railing System (Design No. 2)	47
4.4 Computer Simulation Modeling - Phase II	53
9 FULL-SCALE CRASH TEST - DESIGN NO. 2	54
9.1 TEST LVBR-2 (4,504 lbs (2,043 kg), 30.6 mph (49.2 km/hr), 24.9 degrees)	54
9.2 Test Description	54
9.3 Vehicle Damage	54
9.4 Barrier Damage	55
9.5 Occupant Risk Values	55
10 TEST LVBR-2 DISCUSSION	64
11 CONCLUSIONS	66
12 RECOMMENDATIONS	67
13 REFERENCES	68
14 APPENDICES	71
APPENDIX A - ACCELEROMETER DATA ANALYSIS	71

List of Figures

	Page
1. Static Post Testing Apparatus	11
2. Typical Post Failures	12
3. W-Beam Bridge Railing, Design No. 1	16
4. Flexible W-Beam Bridge Railing System Design Details, Design No. 1	17
5. Test Vehicle, Test LVBR-1	21
6. Vehicle Dimensions, Test LVBR-1	22
7. Test Vehicle, Test LVBR-2	24
8. Vehicle Dimensions, Test LVBR-2	25
9. Vehicle Target Locations, Test LVBR-1	26
10. Vehicle Target Locations, Test LVBR-2	27
11. Location of High-Speed Cameras, Test LVBR-1	30
12. Location of High-Speed Cameras, Test LVBR-2	31
13. Impact Location, Test LVBR-1	35
14. Summary of Test Results and Sequential Photographs, Test LVBR-1	36
15. Additional Sequential Photographs, Test LVBR-1	37
16. Documentary Photographs, Test LVBR-1	38
17. Documentary Photographs, Test LVBR-1	39
18. Documentary Photographs, Test LVBR-1	40
19. Vehicle Position at Rest, Test LVBR-1	41
20. Vehicle Damage, Test LVBR-1	42
21. Bridge Rail Damage, Test LVBR-1	43
22. Bridge Post Damage, Test LVBR-1	44
23. Bridge Post Damage, Test LVBR-1	45
24. Typical Post Failures	50
25. W-Beam Bridge Railing, Design No. 2	51
26. Flexible W-Beam Bridge Railing System Design Details, Design No. 2	52
27. Impact Location, Test LVBR-2	56
28. Summary of Test Results and Sequential Photographs, Test LVBR-2	57
29. Additional Sequential Photographs, Test LVBR-2	58
30. Documentary Photographs, Test LVBR-2	59
31. Documentary Photographs, Test LVBR-2	60
32. Vehicle Position at Rest, Test LVBR-2	61
33. Vehicle Damage, Test LVBR-2	62
34. Typical Bridge Rail and Post Damage, Test LVBR-2	63
A-1. Graph of Longitudinal Deceleration, Test LVBR-1	72
A-2. Graph of Longitudinal Occupant Impact Velocity, Test LVBR-1	73
A-3. Graph of Longitudinal Occupant Displacement, Test LVBR-1	74
A-4. Graph of Lateral Deceleration, Test LVBR-1	75
A-5. Graph of Lateral Occupant Impact Velocity, Test LVBR-1	76
A-6. Graph of Lateral Occupant Displacement, Test LVBR-1	77

A-7. Graph of Longitudinal Deceleration, Test LVBR-2	78
A-8. Graph of Longitudinal Occupant Impact Velocity, Test LVBR-2	79
A-9. Graph of Longitudinal Occupant Displacement, Test LVBR-2	80
A-10. Graph of Lateral Deceleration, Test LVBR-2	81
A-11. Graph of Lateral Occupant Impact Velocity, Test LVBR-2	82
A-12. Graph of Lateral Occupant Displacement, Test LVBR-2	83

List of Tables

	Page
1. AASHTO Crash Test Conditions for Bridge Railings (2) and NCHRP 350 Crash Test Conditions for Longitudinal Barriers (1)	7
2. NCHRP Report 350 Evaluation Criteria for 2000P Pickup Truck Crash Test (1)	9
3. Static Post Testing Results - Phase I	13
4. Static Post Testing Results - Phase II	48
5. Summary of Safety Performance Evaluation	65

1 INTRODUCTION

1.1 Problem Statement

Historically, bridge railing systems have not been developed for use on low-speed, low-volume roads; however, many U.S. Forest Service and National Forest utility and service roads often carry very low traffic volumes at operating speeds of 20 mph (32.2 km/hr) or less. These roads are often narrow, generally incorporating one- or two-lane timber bridges, with span lengths between 15 and 35 ft (4.6 to 10.7 m). The bridge rails that have been designed for high-speed facilities can be unnecessarily expensive for these low-volume road applications. In recognition of the need to develop bridge railings for this low service level, the United States Department of Agriculture (USDA) Forest Service, Forest Product Laboratory (FPL) and Headquarters Engineering Staff, in cooperation with the Midwest Roadside Safety Facility (MwRSF), undertook the task of developing four low-service level bridge railing systems. This report provides a detailed discussion of the research methods used during the development effort for one of the four bridge railings as well as the test results used to evaluate its safety performance.

1.2 Objective

The objective of this research was to develop a low-cost, flexible bridge railing system for use on longitudinal timber decks with low traffic volumes and speeds. Several design factors were considered, such as concerns for aesthetics, economy, material availability, ease of construction, timber deck damage, and structural adequacy. The bridge railing was developed to meet the Test Level 1 (TL-1) evaluation criteria described in the National Cooperative Highway Research Report No. 350, *Recommended Procedures for the Safety Performance Evaluation of Highway Features* (1). A longitudinal glulam timber deck was selected for use in the development of the bridge railing

because it is the weakest type of longitudinal timber deck currently in use for resisting transverse railing loads. Thus, any bridge railing not damaging the longitudinal glulam deck could easily be adapted to other, stronger, timber deck systems.

1.3 Scope

The research objective was achieved by performing several tasks. First, a literature review was performed on existing low performance level railings, as well as bridge railings developed for timber deck bridges. Second, an analysis and design phase was performed on all structural members and connections. Third, static component testing was performed on several post sizes as well as various deck attachment configurations. Fourth, computer simulation modeling was conducted to aid in the analysis and design of the railing system. Fifth, two full-scale vehicle crash tests were performed using a 3/4-ton pickup trucks, weighing approximately 4,409 lbs (2,000 kg), with a target impact speed and angle of 31.1 mph (50 km/h) and 25 degrees, respectively. Finally, the test results were analyzed, evaluated and documented. Conclusions and recommendations were then made that pertain to the safety performance of the flexible bridge railing.

2 LITERATURE REVIEW

2.1 Bridge Railings for Timber Deck Bridges

Over the past seven years, MwRSF and FPL engineers have designed and developed several bridge railings and transitions for use on longitudinal glulam timber bridge decks. Eight bridge railings have been developed for several design impact conditions, including AASHTO Performance Levels 1 and 2 (2), NCHRP 350 Test Levels 1 and 4 (1), as well as for very low-speed, low-volume roadways (3-8). The bridge railing systems developed for timber decks include: (1) an AASHTO PL-1 Glulam Rail with Curb bridge railing (3-6); (2) an AASHTO PL-1 Glulam Rail without Curb bridge railing (3-6); (3) an AASHTO PL-1 Steel Thrie-Beam Rail bridge railing (3-6); (4) an AASHTO PL-2 Steel Thrie-Beam with top-mounted Channel Rail bridge railing (4-7); (5) a NCHRP 350 TL-4 Glulam Rail with Curb bridge railing (4-7); (6) a NCHRP 350 TL-1 low-cost Breakaway W-Beam bridge railing (8); and (7) a Low-Height Curb-Type Sawn Timber bridge railing for low-speed, low-volume roads (8).

Two other research programs conducted in the United States provide information on the crashworthiness of bridge railings for use on timber deck bridges. The first program was performed at Southwest Research Institute (SwRI) in the late 1980's in which crash tests were conducted according to AASHTO Performance Level 1 conditions on a glulam rail with a curb bridge railing system attached to a spike-laminated longitudinal timber bridge deck (9). In 1993, a second research project was conducted by the Constructed Facilities Center (CFC) at West Virginia University with crash testing performed by the Texas Transportation Institute (TTI). Crash tests were performed according to AASHTO Performance Level 1 conditions on three bridge railing systems and one transition system attached to a transverse glulam timber deck (10-13).

2.2 Other W-Beam Bridge Railing Systems

In 1959, researchers at the California Department of Transportation (CALTRANS) crash tested a 12-gauge W-beam bridge railing supported by W6x15.5 steel posts spaced on 6-ft 3-in. (1905-mm) centers (14). The test was performed with a 4,000-lb (1,814-kg) vehicle impacting at 55 mph (89 km/hr) and 30 degrees, resulting in "excessive" rail deflection of approximately 5 ft.

In 1978, TTI researchers crash tested a 12-gauge W-beam bridge railing supported by W6x8.5 steel posts spaced on 6-ft 3-in. (1905-mm) centers (15). The test was performed with a 4,500-lb (2,041-kg) sedan impacting at 60 mph (97 km/hr) and 26.2 degrees and was unsuccessful. The dynamic and permanent set rail deflections were 6 ft and 5 ft, respectively. These large rail deflections allowed the vehicle to wedge between the rail and bridge slab and fracture the bridge posts.

In 1981, SwRI researchers designed and developed a new low-cost bridge railing system using BARRIER VII computer simulation, pendulum component testing, and full-scale vehicle crash testing (16). Nine full-scale vehicle crash tests were conducted with 4,500-lb (2,041-kg) sedans and one 20,000-lb (9,072-kg) school bus. The railing system consisted of a three beam supported by either wood or steel posts spaced on 8-ft 4-in. (2,540-mm) centers. This bridge rail concept exhibited behavior that was dramatically different from previous bridge railing research projects. Although large deflections and subsequent vehicle movement below the bridge deck had occurred, they did not result in failure of the railing system to contain and redirect the vehicle. The significance of rail tension and post behavior was also demonstrated. Without adequate tensile capacity and splice capacity, the railing would not have contained the vehicles. Post separation from the deck support and beam prior to the occurrence of large deflections assured that wheel snagging would not occur.

3 TEST REQUIREMENTS AND EVALUATION CRITERIA

3.1 Test Requirements

Until recently, bridge railings were typically designed to satisfy the requirements provided in the American Association of State Highway and Transportation Officials' (AASHTO's) *Guide Specifications for Bridge Railings* (2). More specifically, bridge railings were designed according to the appropriate performance level of the roadway, based upon a number of factors such as design speed, average daily traffic (ADT), percentage of trucks, bridge rail offset, and number of lanes. These guide specifications included three performance levels, as shown in Table 1, which provided criteria for evaluating the safety performance of bridge railings.

The recently published NCHRP Report No. 350 (1) provides for six test levels, as shown in Table 1, for evaluating longitudinal barriers. Although this document does not contain objective criteria for the conditions under which each test level is to be used, safety hardware developed to meet the lower test levels are generally intended for use on lower service level roadways while higher test level hardware is intended for use on higher service level roadways. The lowest performance level, Test Level 1 (TL-1), is suitable for applications on low-volume, low-speed facilities such as residential streets. Thus, test impact conditions from Test Level 1 were chosen for this flexible bridge railing. Test Level 1 requires that the bridge railing meet two full-scale vehicle crash tests: (1) an 1,808-lb (820-kg) small car impacting at 31.1 mph (50 km/hr) and 20 degrees; and (2) a 4,409-lb (2,000-kg) pickup truck impacting at a speed of 31.1 mph (50 km/hr) and 25 degrees. However, the 1,808-lb (820-kg) small car crash test was considered unnecessary, since there was no potential for occupant risk problems arising from wheel snagging caused by the weak timber posts and low impact speed. In addition, W-beam barrier systems have been shown to meet safety

performance standards when impacted by small cars at impact speeds up to 60 mph (96.6 km/hr) (17-
18).

Table 1. AASHTO Crash Test Conditions for Bridge Railings (2) and NCHRP 350 Crash Test Conditions for Longitudinal Barriers (1)

AASHTO Performance Level (2)	Impact Conditions				
	Small Car (816 kg)	Pickup Truck (2,449 kg)	Medium Single-Unit Truck (8,165 kg)	Van-Type Tractor-Trailer (22,680 kg)	
1	80.5 km/h & 20 deg	72.4 km/h & 20 deg			
2	96.6 km/h & 20 deg	96.6 km/h & 20 deg	80.5 km/h & 15 deg		
3	96.6 km/h & 20 deg	96.6 km/h & 20 deg		80.5 km/h & 15 deg	
NCHRP 350 Test Level (1)	Impact Conditions				
	Small Car (820 kg)	Pickup Truck (2,000 kg)	Single-Unit Van Truck (8,000 kg)	Tractor/Van Trailer (36,000 kg)	Tractor/Tank Trailer (36,000 kg)
1	50 km/h & 20 deg	50 km/h & 25 deg			
2	70 km/h & 20 deg	70 km/h & 25 deg			
3 (Basic Level)	100 km/h & 20 deg	100 km/h & 25 deg			
4	100 km/h & 20 deg	100 km/h & 25 deg	80 km/h & 15 deg		
5	100 km/h & 20 deg	100 km/h & 25 deg		80 km/h & 15 deg	
6	100 km/h & 20 deg	100 km/h & 25 deg			80 km/h & 15 deg

3.2 Evaluation Criteria

Evaluation criteria for full-scale vehicle crash testing are based on three appraisal areas: (1) structural adequacy; (2) occupant risk; and (3) vehicle trajectory after collision. Criteria for structural adequacy are intended to evaluate the ability of the railing to contain, redirect, or allow controlled vehicle penetration in a predictable manner. Occupant risk evaluates the degree of hazard to occupants in the impacting vehicle. Vehicle trajectory after collision is a measure of the potential for the post-impact trajectory of the vehicle to cause subsequent multi-vehicle accidents, thereby subjecting occupants of other vehicles to undue hazard or to subject the occupants of the impacting vehicle to secondary collisions with other fixed objects. These three evaluation criteria are defined in Table 2.

Table 2. NCHRP Report 350 Evaluation Criteria for 2000P Pickup Truck Crash Test (1).

Structural Adequacy	A. Test article should contain and redirect the vehicle; the vehicle should not penetrate, underride, or override the installation although controlled lateral deflection of the test article is acceptable.
Occupant Risk	D. Detached elements, fragments or other debris from the test article should not penetrate or show potential for penetrating the occupant compartment, or present an undue hazard to other traffic, pedestrians, or personnel in a work zone. Deformations of, or intrusions into, the occupant compartment that could cause serious injuries should not be permitted.
	F. The vehicle should remain upright during and after collision although moderate roll, pitching, and yawing are acceptable.
Vehicle Trajectory	K. After collision it is preferable that the vehicle's trajectory not intrude into adjacent traffic lanes.
	L. The occupant impact velocity in the longitudinal direction should not exceed 12 m/sec and the occupant ridedown acceleration in the longitudinal direction should not exceed 20 G's.
	M. The exit angle from the test article preferably should be less than 60 percent of test impact angle, measured at time of vehicle loss of contact with test device.

4 RAIL SYSTEM DEVELOPMENT - PHASE I

4.1 Design Considerations

A steel W-beam railing with timber bridge posts was selected for use in the flexible bridge railing design based on previously crash tested metal beam bridge railings (14-16), economics, and material availability. Breakaway posts, rather than stiff posts, were chosen so that no damage would occur to the timber deck or connection hardware and to keep material costs below \$10/ft (\$33/m) by reducing the required structural capacity of the post-to-deck attachment. A side-mounted post-to-deck attachment with no rail/post blockouts was selected in order to reduce the required width of timber deck.

4.2 Static Post Testing - Phase I

Static post testing was used to determine the force-deflection characteristics of two dimension lumber post sizes, 4-in. by 4-in. (102-mm by 102-mm) and 4-in. by 6-in. (102-mm by 152-mm) nominal. The cantilevered posts were bolted between two steel angles and attached to a rigid plate, as shown in Figure 1. Various angle sizes were used during the testing in order to determine the optimum angle dimensions.

Thirteen static tests were performed and are summarized in Table 3. Typical damage to the timber post specimens is shown in Figure 2. A 4-in. by 6-in. (102-mm by 152-mm) dimension lumber post measuring 33-in. (838-mm) long with steel angles measuring 5 in. by 5 in. by $\frac{3}{8}$ in. (127 mm by 127 mm by 10 mm) was selected for use in the bridge railing system. The 4-in. by 6-in. (102-mm by 152-mm) lumber post rather than the 4-in. by 4-in. (102-mm by 102-mm) lumber post was chosen because it provided increased structural capacity while not allowing damage to occur to the post-to-deck attachment hardware or the timber deck. In addition, the researchers reasoned that

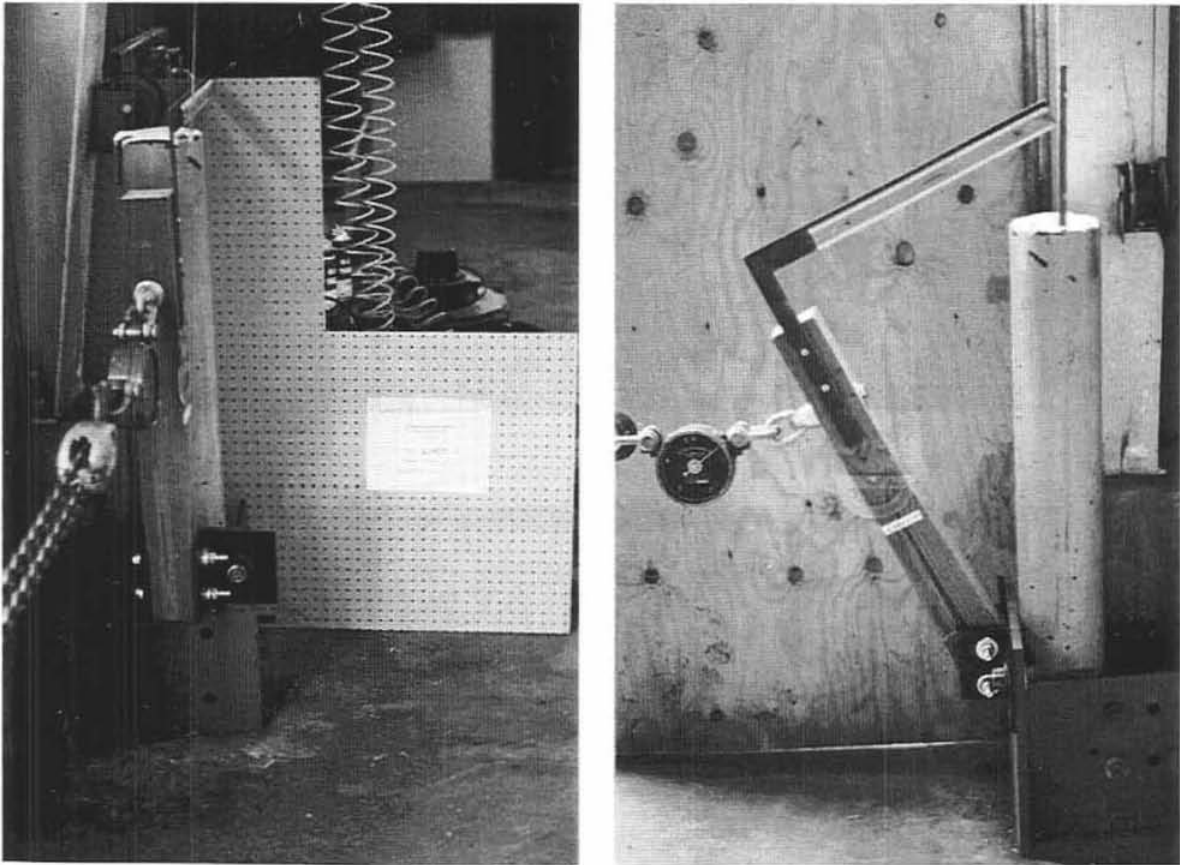


Figure 1. Static Post Testing Apparatus

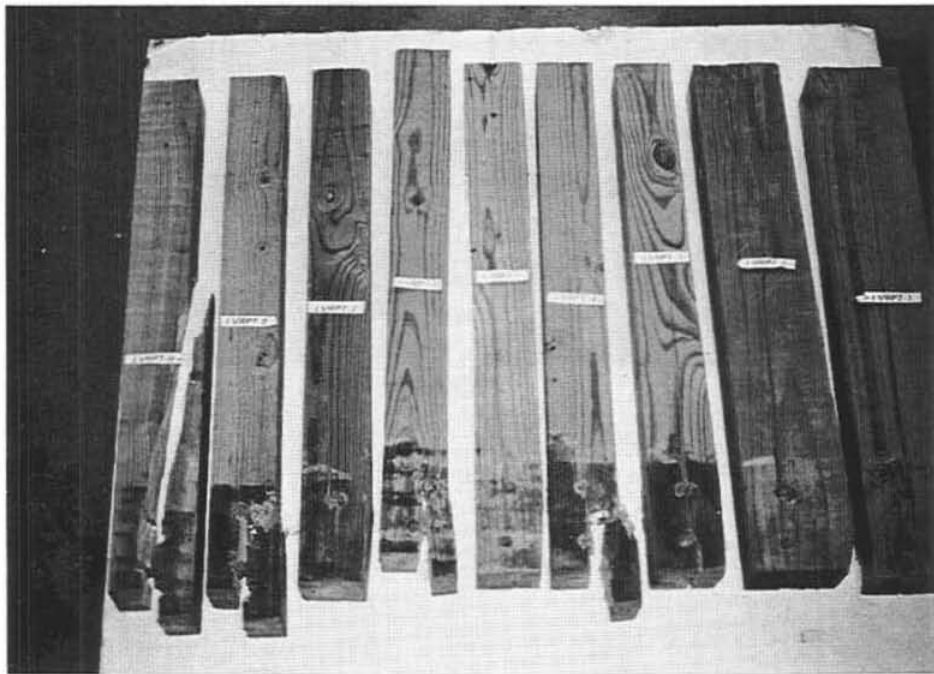
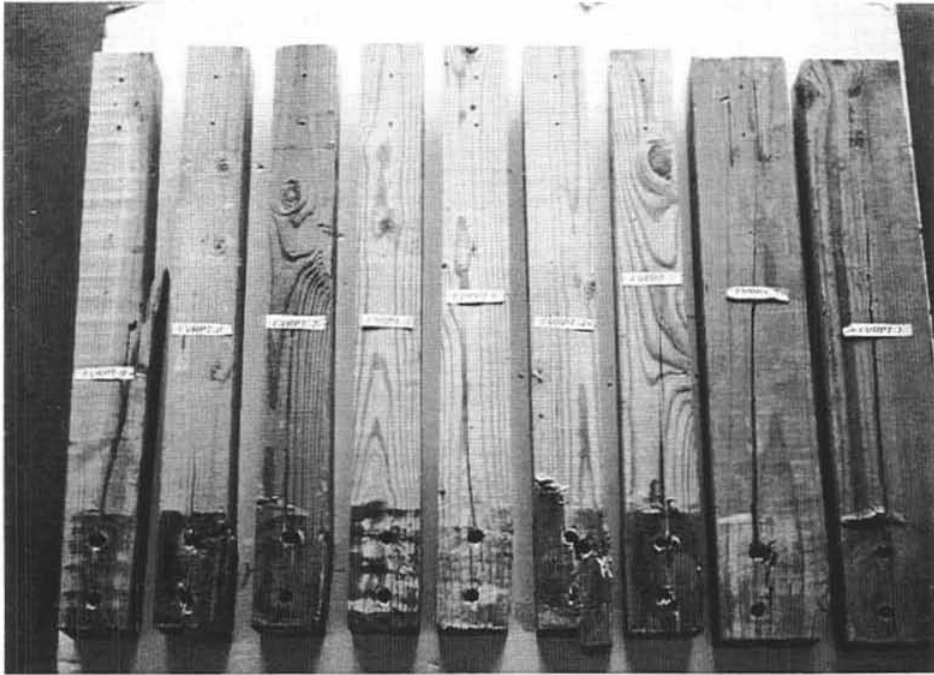


Figure 2. Typical Post Failures

Table 3. Static Post Testing Results - Phase I

Test No.	Hardware Sizes		Bolt Torque (ft-lbs)	Peak Load (lbs)	Deflection @ Peak Load (in.)
	Timber Post	Steel Angles			
LVRRT-1	4 x 6	6 x 6 x 7/16	75	2400	11.7
LVRPT-2	4 x 6	6 x 6 x 7/16	75	1700	13.1
LVRPT-3	4 x 4	6 x 6 x 7/16	75	875	4.7
LVRPT-4	4 x 4	6 x 6 x 7/16	75	1125	5.3
LVRPT-5	4 x 4	6 x 6 x 7/16	25	1140	4.0
LVRPT-6	4 x 4	4 x 6 x ½	75	1500	5.2
LVRPT-7	4 x 4	4 x 6 x ½	75	1300	6.6
LVRPT-8	4 x 4	3½ x 5 x ¼	75	1100	2.6
LVRPT-9	4 x 4	3½ x 5 x ¼	75	1200	2.8
LVRPT-10	4 x 6	5 x 5 x 5/16	75	2400	8.9
T-1	4 x 4	4 x 6 x ½	75	1250	5.5
T-2	4 x 4	3½ x 5 x ¼	75	875	2.2
T-3	4 x 6	6 x 6 x 7/16	75	2375	10.7

the larger post size would have less of a perception problem where the posts would be considered to be too “weak” by motorists, bridge engineers, and construction workers. The maximum static force for the 4-in. by 6-in. (102-mm by 152-mm) post size was 2.4 kips (10.7 kN), while the maximum static force for the 4-in. by 4-in. (102-mm by 102-mm) post size was found to be 1.5 kips (6.7 kN), as shown in Table 3. The 5 in. by 5 in. by $\frac{3}{8}$ in. (127 mm by 127 mm by 10 mm) steel angle size was also selected to minimize damage to the post-to-deck attachment hardware and the timber deck.

4.3 Design Details

4.3.1 Timber Deck and Substructure

A full-size simulated timber bridge system was constructed at the MwRSF outdoor test site. In order to simulate an actual timber bridge installation, the longitudinal glulam timber bridge deck was mounted on six reinforced-concrete bridge supports. The inner three concrete bridge supports had center-to-center spacings of 18 ft 9 in. (5.72 m) whereas the outer two spacings were 18 ft 3 in. (5.56 m).

The longitudinal glulam timber deck consisted of ten rectangular panels. The panels measured 3-ft 11⁷/₈-in. (1.22-m) wide by 18-ft 8¹/₂-in. (5.70-m) long by 10³/₄-in. (273-mm) thick. The timber deck was constructed so that two panels formed the width of the deck and five panels formed the length of the deck. The longitudinal glulam timber deck was fabricated with West Coast Douglas Fir and treated with pentachlorophenol in heavy oil to a minimum net retention of 0.6 lbs/ft³ (9.61 kg/m³) as specified in AWWA Standard C14 (19). At each longitudinal midspan location of the timber deck panels, stiffener beams were bolted transversely across the bottom side of the timber deck panels per AASHTO bridge design requirements. The stiffener beams measured 5¹/₈-in. (130-mm) wide by 6-in. (152-mm) thick by 8-ft (2.44-m) long. In addition, a 2-in. (51-mm) asphalt wearing surface was placed on the top of the timber deck in order to represent actual field conditions.

4.3.2 Flexible W-Beam Bridge Railing System (Design No. 1)

The total length of the test installation was 200 ft (60.96 m), as shown in Figures 3 through 4. The flexible, side-mounted W-beam bridge railing system consisted of three major structural components: (1) W-beam guardrail; (2) timber posts; and (3) steel angle post-to-deck attachment hardware. Detailed drawings of the bridge rail components are provided in Figure 3. Photographs

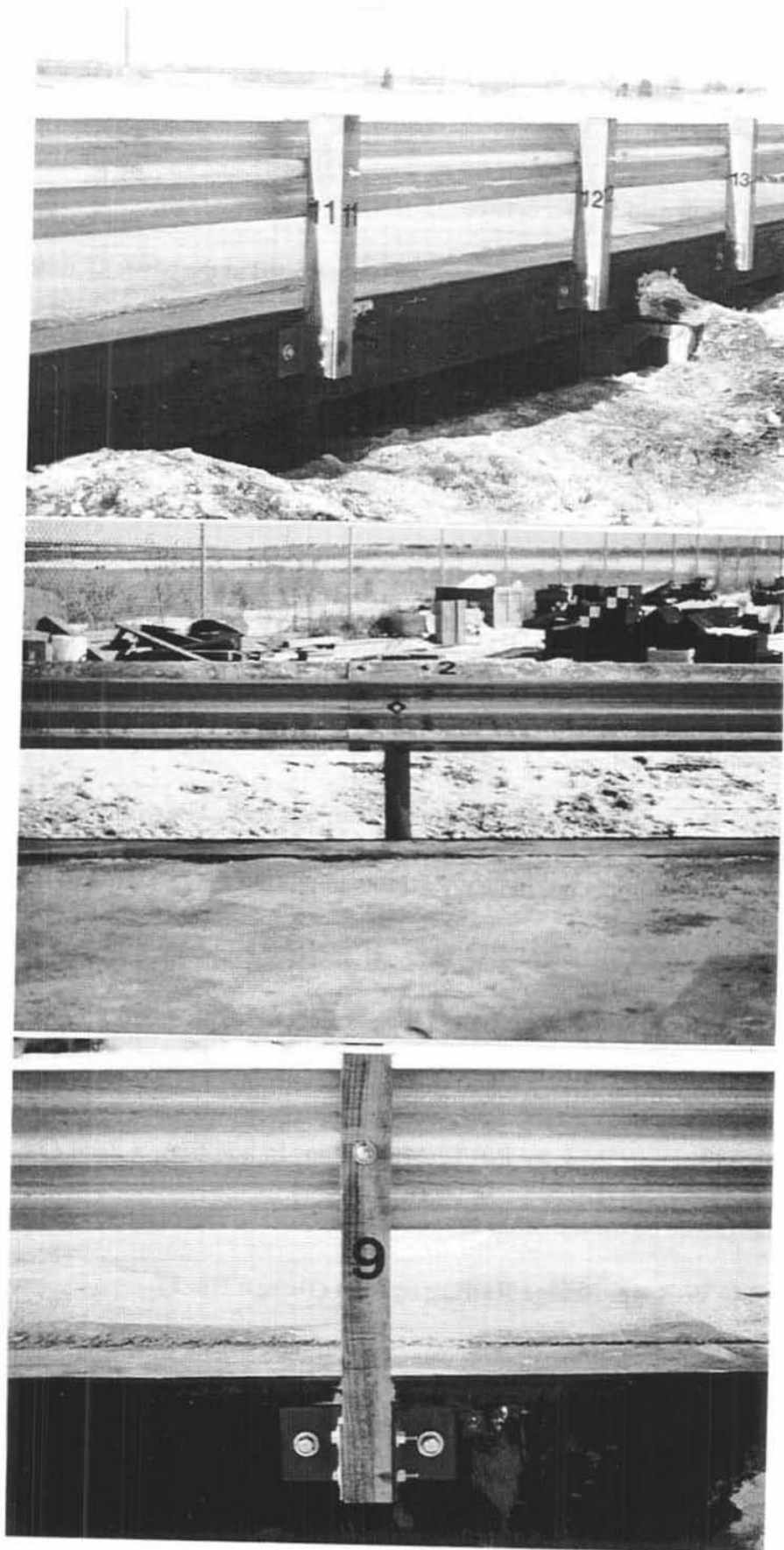


Figure 3. W-Beam Bridge Railing, Design No. 1

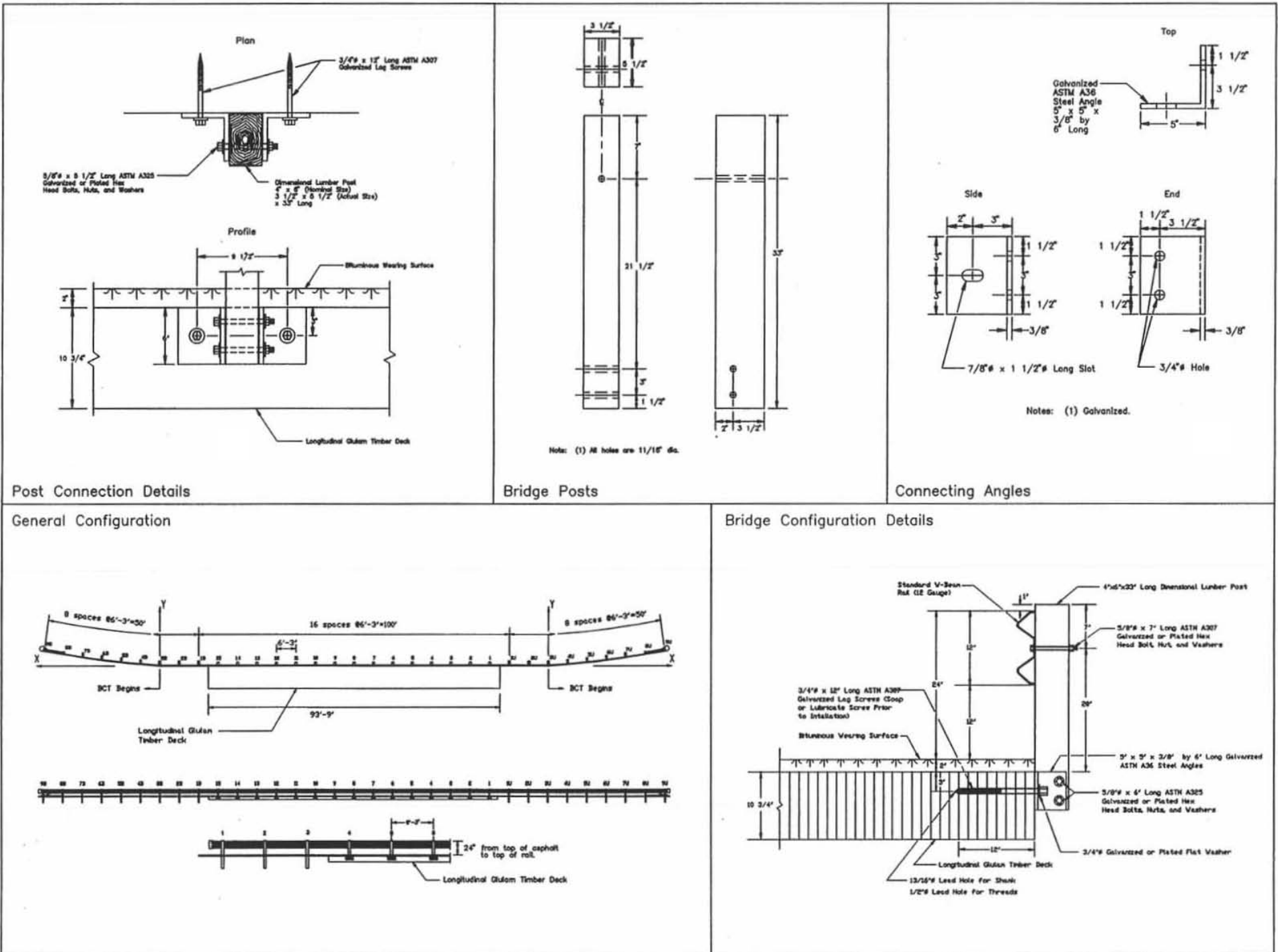


Figure 4. Flexible W-Beam Bridge Railing System Design Details, Design No. 1

of the bridge railing system are shown in Figure 4.

A standard 12-gauge (2.66-mm) W-beam rail was selected for the rail element with a 24-in. (610-mm) top mounting height, as measured from the top of the asphalt wearing surface to the center of the rail. The 100-ft (30.48-m) long bridge rail was supported by fifteen posts spaced on 6-ft 3-in. (1905-mm) centers. The chromated copper arsenate (CCA) treated, dimension lumber posts measured 4-in. by 6-in. (102-mm by 152-mm) nominal or 3.5-in. by 5.5-in. (89-mm by 140-mm) actual dressed size. The lumber posts were manufactured using Douglas Fir Grade No. 2 or better. A $\frac{5}{8}$ -in. (15.9-mm) diameter by 7-in. (178-mm) long ASTM A307 galvanized hex head bolt attached the rail to each post. Each post was placed between two 5-in. by 5-in. by $\frac{3}{8}$ -in. (127-mm by 127-mm by 9.5-mm) galvanized steel angles measuring 6-in. (152-mm) in length. Two $\frac{5}{8}$ -in. (15.9-mm) diameter by 5½-in. (140-mm) long ASTM A325 galvanized hex head bolts attached the post between the angles. Each post with attached angles was rigidly fixed to the outside vertical surface of the timber deck with two $\frac{3}{4}$ -in. (19.0-mm) diameter by 12-in. (305-mm) long ASTM A307 galvanized lag screws.

Approach guardrails were placed on each end of the bridge railing. Each W-Beam approach guardrail was 50-ft (15.24-m) long and supported by 6-in. by 8-in. (152-mm by 203-mm) timber posts spaced on 6-ft 3-in. (1905-mm) centers. Guardrail anchorage was provided at each end by a modified breakaway cable terminal (MBCT) with steel foundation tubes, bearing plates, and channel struts.

4.4 Computer Simulation Modeling - Phase I

Computer simulation modeling with BARRIER VII was then performed on Design No. 1 to analyze the dynamic performance of the bridge railing prior to full-scale crash testing (20).

BARRIER VII computer simulation has been used extensively to model vehicle-barrier collisions; however, the 2-dimensional computer program does not have the ability to predict vehicle climbing and vaulting over longitudinal barriers.

Computer simulation was conducted modeling a 1,996-kg (4,400-lb) pickup truck impacting at 31 mph (50 km/h) and 25 degrees according to Test Level 1 of NCHRP Report No. 350 (1). The simulation results indicated that the flexible bridge railing design satisfactorily redirected the 1,996-kg (4,400-lb) pickup truck. For Design No. 1, computer simulation predicted that five timber posts would be broken during impact, and the maximum dynamic deflection of the W-Beam would be 26.0 in. (660 mm). In addition, the predicted peak 0.050-sec average impact force perpendicular to the bridge railing was approximately 7.3 kips (32.5 kN).

5 TEST CONDITIONS

5.1 Test Facility

The testing facility is located at the Lincoln Air-Park on the NW end of the Lincoln Municipal Airport and is approximately 5 mi (8.0 km) NW of the University of Nebraska-Lincoln. The site is protected by an 8-ft (2.44-m) high chain-link security fence.

5.2 Vehicle Tow and Guidance System

A reverse cable tow system with a 1:2 mechanical advantage was used to propel the test vehicles. The distance traveled and the speed of the tow vehicle are one-half that of the test vehicle. The test vehicle was released from the tow cable before impact with the bridge rail. A fifth wheel, built by the Nucleus Corporation, was located on the tow vehicle and used in conjunction with a digital speedometer to increase the accuracy of the test vehicle impact speed.

A vehicle guidance system developed by Hinch (21) was used to steer the test vehicle. A guide-flag, attached to the front-left wheel and the guide cable, was sheared off before impact. The 3/8-in. (9.5-mm) diameter guide cable was tensioned to approximately 3,000 lbs (13.3 kN), and supported laterally and vertically every 100 ft (30.48 m) by hinged stanchions. The hinged stanchions stood upright while holding up the guide cable, but as the vehicle was towed down the line, the guide-flag struck and knocked each stanchion to the ground. The vehicle guidance system was approximately 400-ft (122-m) long.

5.3 Test Vehicles

For test LVBR-1, a 1984 Chevrolet C-20 ¾-ton pickup truck was used as the test vehicle. The test inertial and gross static weights were 4,499 lbs (2,041 kg). The test vehicle is shown in Figure 5, and vehicle dimensions are shown in Figure 6.

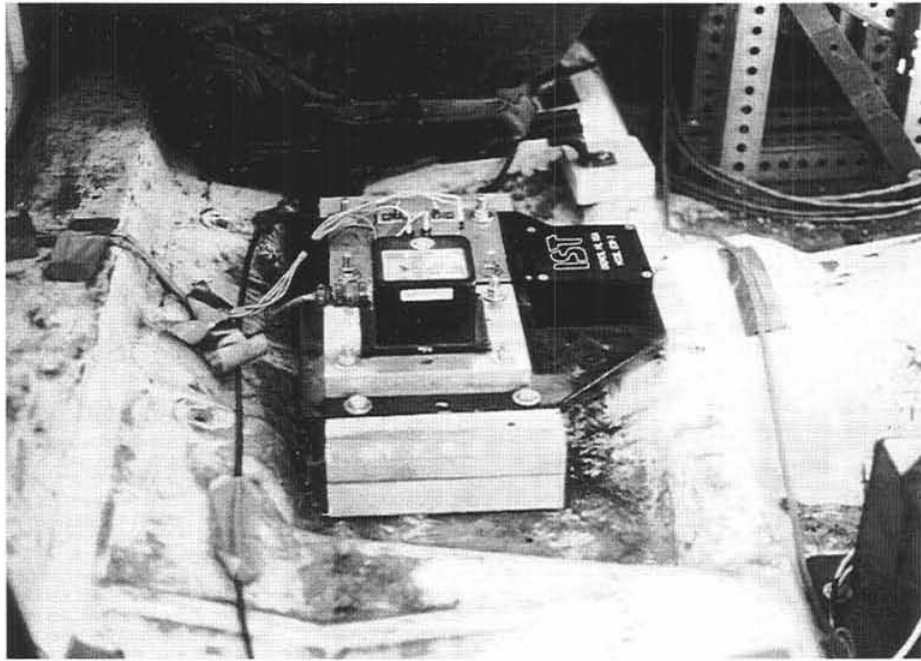
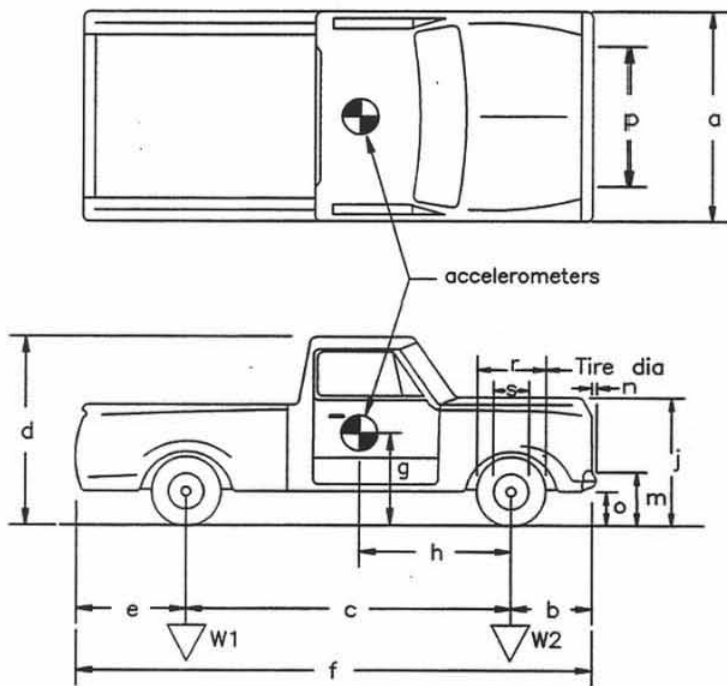


Figure 5. Test Vehicle, Test LVBR-1

Date: 2/4/94 Test Number: LVBR-1 Model: C-20
 Make: Chevrolet Vehicle I.D.#: 1G3GC24M7ES100123
 Tire Size: P235/85-R16(F) Year: 1984 Odometer: NA
P245/85-R16(R)



Vehicle Geometry - in

a	<u>77.5</u>	b	<u>31.0</u>
c	<u>132.0</u>	d	<u>72.0</u>
e	<u>53.0</u>	f	<u>216.0</u>
g	<u>28.5</u>	h	<u>57.3</u>
i	<u>---</u>	j	<u>44.5</u>
k	<u>---</u>	l	<u>---</u>
m	<u>27.75</u>	n	<u>4.0</u>
o	<u>19.25</u>	p	<u>65.75</u>
r	<u>31.0</u>	s	<u>17.5</u>

Engine Type V-8
 Engine Size 350 cu. in.

Transmission Type:
 Automatic or Manual
 FWD or RWD or 4WD

Weight - lbs	Curb	Test Inertial	Gross Static
W1	<u>1835</u>	<u>1953</u>	<u>1953</u>
W2	<u>2375</u>	<u>2546</u>	<u>2546</u>
Wtotal	<u>4210</u>	<u>4499</u>	<u>4499</u>

Figure 6. Vehicle Dimensions, Test LVBR-1

For test LVBR-2, a 1985 Chevrolet C-20 $\frac{3}{4}$ -ton pickup truck was used as the test vehicle. The test inertial and gross static weights were 4,504 lbs (2,043 kg). The test vehicle is shown in Figure 7, and vehicle dimensions are shown in Figure 8.

The Elevated Axle Method (22) was used to determine the vertical component of the center of gravity. This method converts measured wheel weights at different elevations to the location of the vertical component of the center of gravity. The longitudinal component of the center of gravity was determined using the measured axle weights. The location of the final centers of gravity are shown in Figures 6 and 8.

Square, black and white-checked targets were placed on the vehicle to aid in the analysis of the high-speed film, as shown in Figures 5, 7, 9 and 10. One target was placed on the center of gravity at the driver's side door and on the roof of the vehicle. The remaining targets were located for reference so that they could be viewed from the high-speed cameras for film analysis.

The front wheels of the test vehicle were aligned for camber, caster, and toe-in values of zero so that the vehicles would track properly along the guide cable. Two 5B flash bulbs were mounted on the hood of the vehicles to pinpoint the time of impact with the bridge railing on the high-speed film. The flash bulbs were fired by a pressure tape switch mounted on the front face of the bumper. A remote controlled brake system was installed in the test vehicle so the vehicle could be brought safely to a stop after the test.

5.4 Data Acquisition Systems

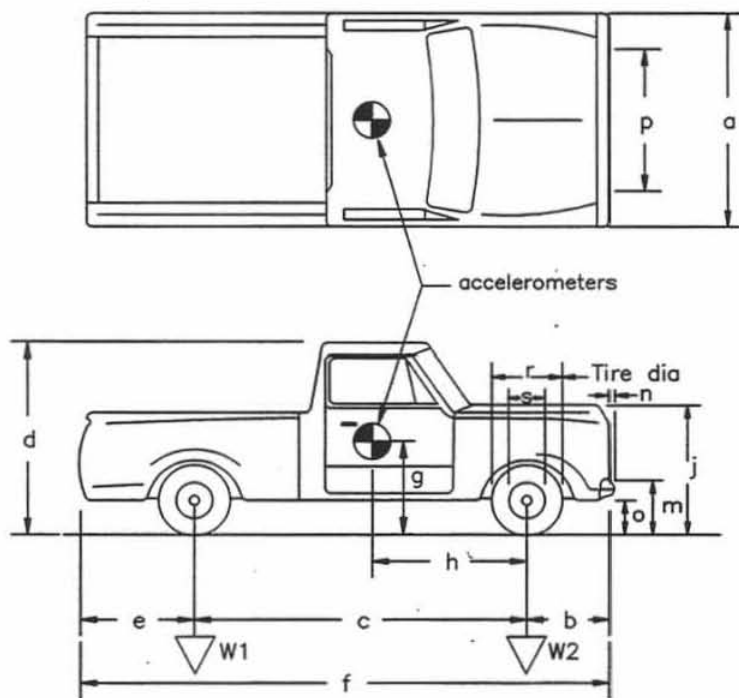
5.4.1 Accelerometers

Two triaxial piezoresistive accelerometer systems with a range of ± 200 g's (Endevco Model 7264) were used to measure the acceleration in the longitudinal, lateral, and vertical directions. Two



Figure 7. Test Vehicle, Test LVBR-2

Date: 3/18/94 Test Number: LVBR-2 Model: C-20
 Make: CHEVROLET Vehicle I.D.#: 1GCGC24MXF311219
 Tire Size: P235/85-R16 Year: 1985 Odometer: 132989



Vehicle Geometry - inches

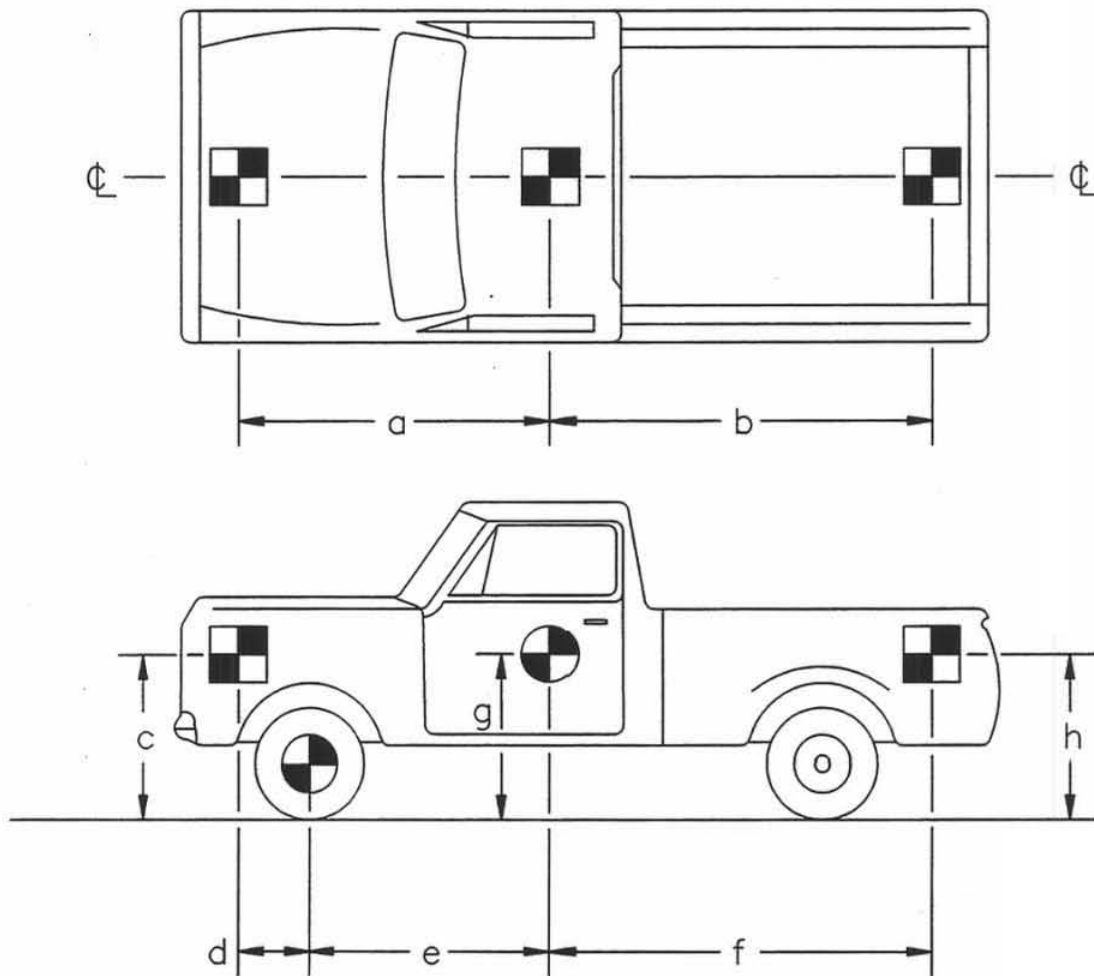
a	<u>78.0</u>	b	<u>32.0</u>
c	<u>131.5</u>	d	<u>73.0</u>
e	<u>51.0</u>	f	<u>214.0</u>
g	<u>29.0</u>	h	<u>57.5</u>
i	<u>---</u>	j	<u>50.0</u>
k	<u>---</u>	l	<u>---</u>
m	<u>27.0</u>	n	<u>4.0</u>
o	<u>16.0</u>	p	<u>65.5</u>
r	<u>30.5</u>	s	<u>17.5</u>

Engine Type V-8
 Engine Size 350 cu. in.

Transmission Type:
 Automatic or Manual
 FWD or RWD or 4WD

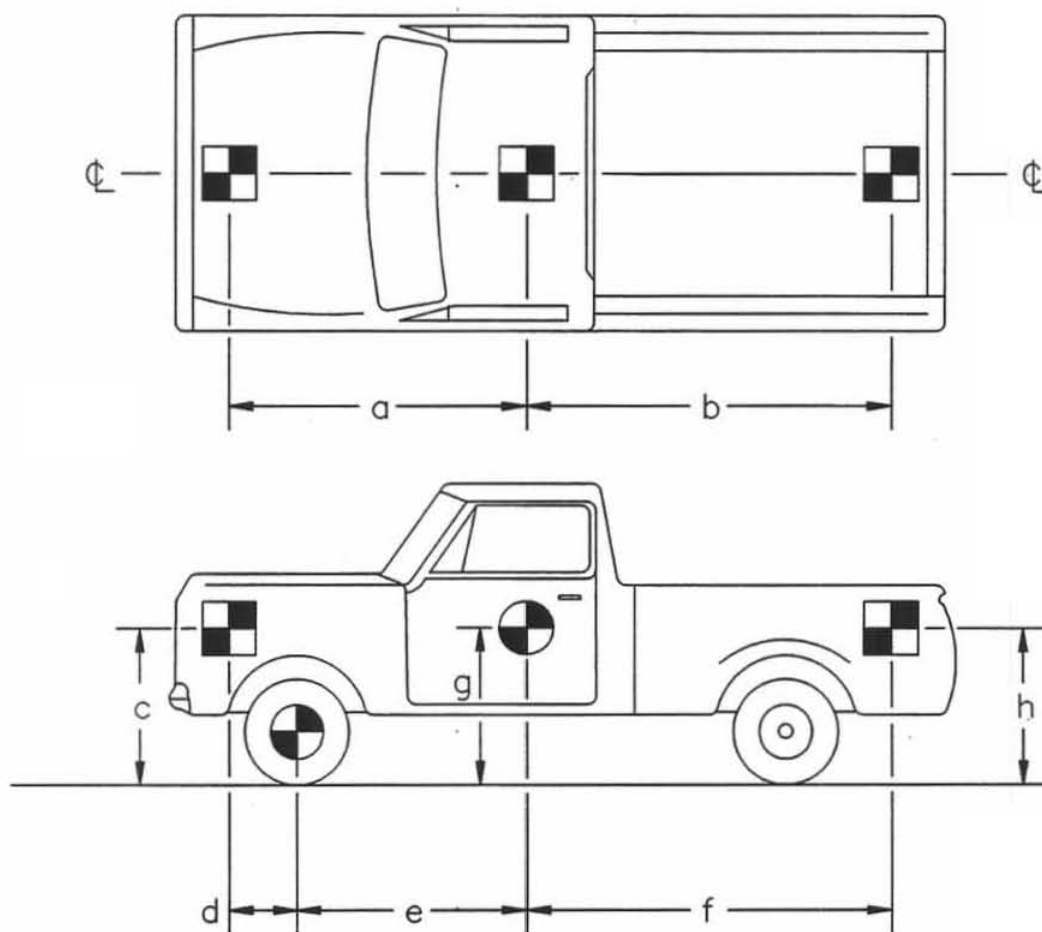
Weight - lbs	Curb	Test Inertial	Gross Static
W1	<u>1900</u>	<u>1963</u>	<u>1963</u>
W2	<u>2430</u>	<u>2541</u>	<u>2541</u>
Wtotal	<u>4330</u>	<u>4504</u>	<u>4504</u>

Figure 8. Vehicle Dimensions, Test LVBR-2



TEST No.: <u>LVBR-1</u>							
TARGET GEOMETRY							
INCHES							
a	<u>57.3</u>	c	<u>41.0</u>	e	<u>57.3</u>	g	<u>28</u>
b	<u>96.0</u>	d	<u>0</u>	f	<u>96</u>	h	<u>40.75</u>

Figure 9. Vehicle Target Locations, Test LVBR-1



TEST No.: <u>LVBR-2</u>							
TARGET GEOMETRY							
INCHES							
a	<u>57.5</u>	c	<u>42</u>	e	<u>57.5</u>	g	<u>29</u>
b	<u>96</u>	d	<u>0</u>	f	<u>96</u>	h	<u>42</u>

Figure 10. Vehicle Target Locations, Test LVBR-2

accelerometers were mounted in each of the three directions and were rigidly attached to a metal block mounted at the center of gravity. Accelerometer signals were received and conditioned by an onboard Series 300 Multiplexed FM Data System built by Metraplex Corporation. The multiplexed signal was then transmitted to the Honeywell 101 Analog Tape Recorder. Computer software, "EGAA" and "DADiSP" were used to digitize, analyze, and plot the accelerometer data.

A backup triaxial piezoresistive accelerometer system with a range of ± 200 G's was also used to measure the acceleration in the longitudinal, lateral, and vertical directions at a sample rate of 3,200 Hz. The environmental shock and vibration sensor/recorder system, Model EDR-3, was developed by Instrumented Sensor Technology (IST) of Okemos, Michigan. The EDR-3 was configured with 256 Kb of RAM memory and a 1,120 Hz filter. Computer software, "DynaMax 1 (DM-1)" and "DADiSP" were used to digitize, analyze, and plot the accelerometer data.

5.4.2 Rate Transducer

A Humphrey 3-axis rate transducer with a range of 250 deg/sec in each of the three directions (pitch, roll, and yaw) was used to measure the rates of motion of the test vehicle. The rate transducer was rigidly attached to the vehicles near the center of gravity of the test vehicle. Rate transducer signals were received and conditioned by an onboard Series 300 Multiplexed FM Data System built by Metraplex Corporation. The multiplexed signal was then transmitted by radio telemetry to a Honeywell 101 Analog Tape Recorder. Computer software, "EGAA" and "DADiSP" were used to digitize, analyze, and plot the rate transducer data.

5.4.3 High-Speed Photography

For test LVBR-1, five high-speed 16-mm cameras, with operating speeds of approximately 500 frames/sec, were used to film the crash test. A Red Lake Locam with a wide-angle 12.5-mm lens was placed above the test installation to provide a field of view perpendicular to the ground. A Red Lake Locam with a 76-mm lens was placed downstream from the impact point and had a field of view parallel to the bridge rail. A Photec IV with a 55-mm lens was placed on the traffic side of the bridge rail and had a field of view perpendicular to the bridge rail. A Red Lake Locam was placed upstream from the impact point and had a field of view parallel to the bridge rail. A Red Lake Locam was placed downstream and behind the bridge rail. A schematic of all five camera locations for test LVBR-1 is shown in Figure 11.

For test LVBR-2, four high-speed 16-mm cameras, with operating speeds of approximately 500 frames/sec, were used to film the crash test. A Red Lake Locam with a wide-angle 12.5-mm lens was placed above the test installation to provide a field of view perpendicular to the ground. A Red Lake Locam and a Photec IV, with a 76-mm and 80-mm lens, respectively, were placed downstream from the impact point and had a field of view parallel to the bridge rail. A Photec IV with a 55-mm lens was placed on the traffic side of the bridge rail and had a field of view perpendicular to the bridge rail. A schematic of all five camera locations for test LVBR-2 is shown in Figure 12.

A 30-ft (9.14-m) long by 15-ft (4.57-m) wide, white-colored grid was painted on the asphalt surface on the traffic side of the bridge rail. This grid was incremented in 5-ft (1.52-m) divisions to provide a visible reference system for use in the analysis of the overhead high-speed film. The film was analyzed using the Vanguard Motion Analyzer. Actual camera speed and camera divergence factors were considered in the analysis of the high-speed film.

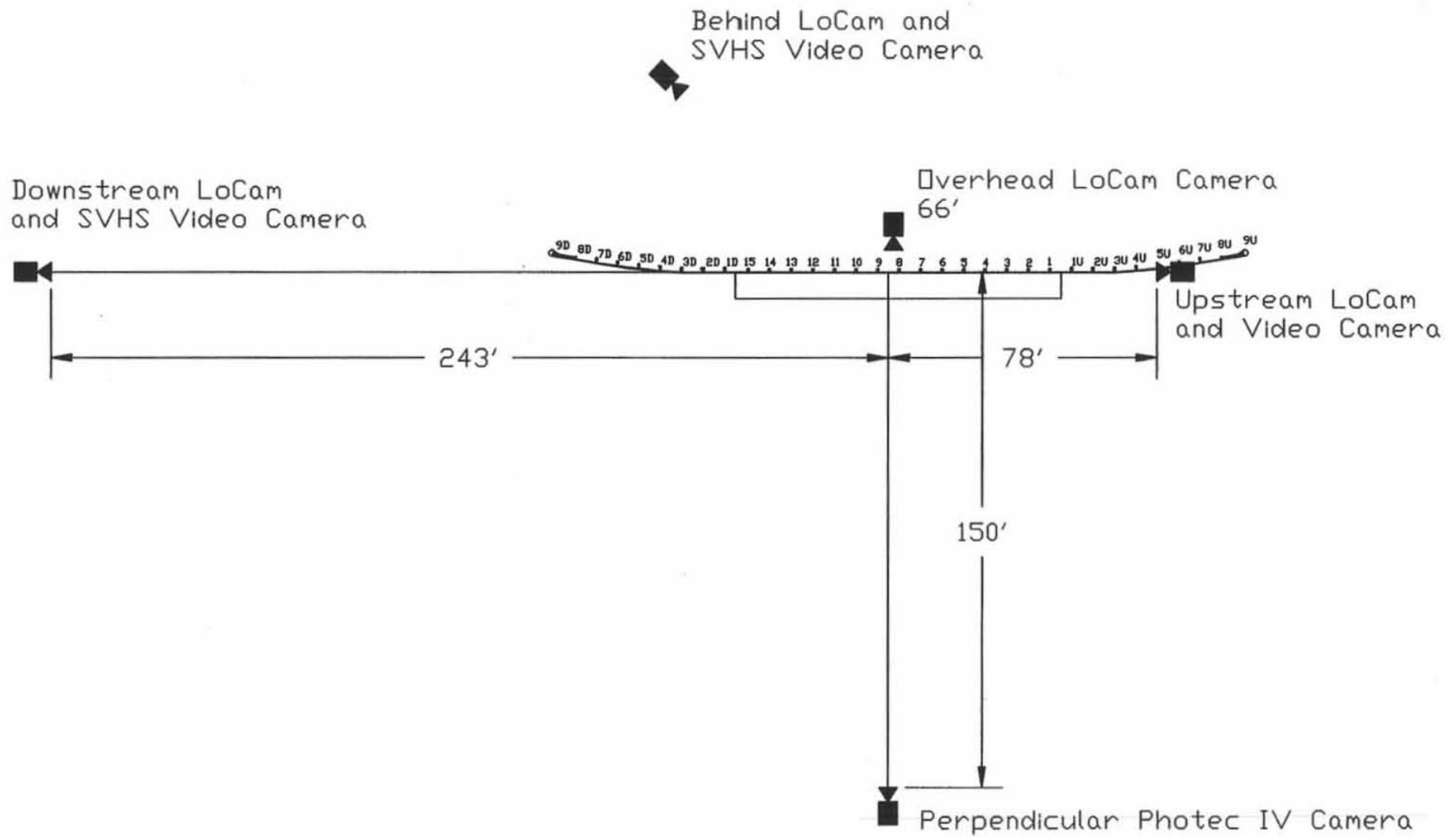


Figure 11. Location of High-Speed Cameras, Test LVBR-1

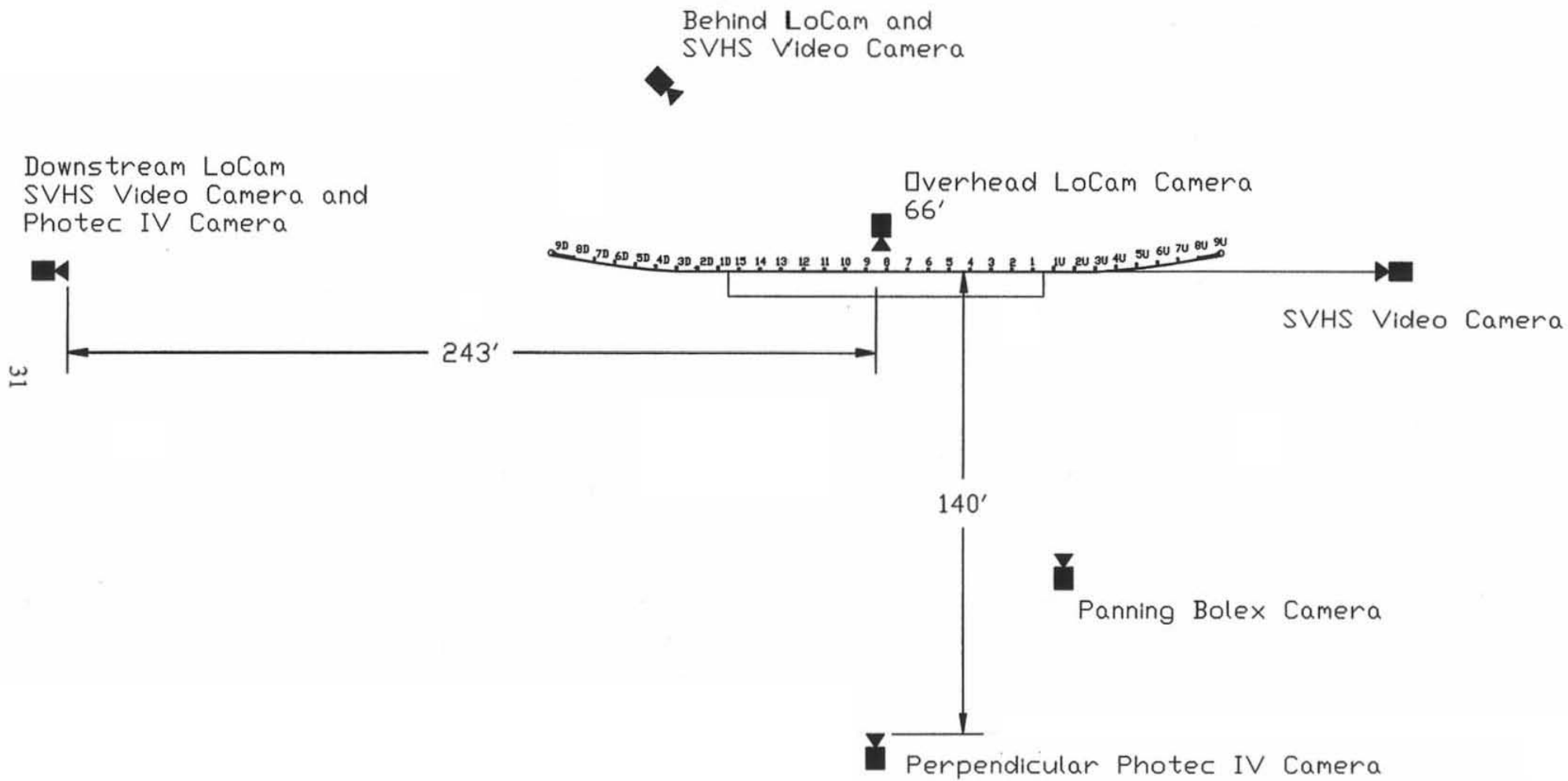


Figure 12. Location of High-Speed Cameras, Test LVBR-2

5.4.4 Pressure Tape Switches

For test LVBR-1, six pressure-activated tape switches, spaced at 5-ft (1.52-m) intervals, were used to determine the speed of the vehicle before impact. For test LVBR-2, three pressure-activated tape switches, spaced at 3-ft (0.91-m) intervals, were used to determine the speed of the vehicle before impact. Each tape switch fired a strobe light which sent an electronic timing signal to the data acquisition system as the left front tire of the test vehicle passed over it. Test vehicle speeds were determined from electronic timing mark data recorded on "EGAA" software. Strobe lights and high-speed film analysis are used only as a backup in the event that vehicle speeds cannot be determined from the electronic data.

6 FULL-SCALE CRASH TEST - DESIGN NO. 1

6.1 Test LVBR-1 (4,499 lbs (2,041 kg), 31.2 mph (50.2 km/hr), 26.8 degrees)

A 1984 Chevrolet C-20 pickup truck impacted the W-beam bridge railing at post no. 7, as shown in Figure 13. A summary of the test results and the sequential photographs is presented in Figure 14. Additional sequential photographs are shown in Figure 15. Documentary photographs of the crash test are shown in Figures 16 through 18.

6.2 Test Description

Upon impact, the right-side of the vehicle's front bumper contacted the point of the top corrugation of the W-beam rail and traveled longitudinally along the rail for a short distance. The vehicle's bumper traveled diagonally up the slope of the top corrugation and then continued to travel longitudinally along the rail contacting just below the top. The steel rim of the vehicle's right-front tire contacted the point of the lower corrugation of the W-beam rail and gouged into the rail leaving a horizontal depression. However, at the end of this gouge in the lower corrugation, the vehicle's tire and rim began to travel upward slightly, as evidenced by the depression sloping upward.

Following the upward motions of both the front bumper and right-front tire, the vehicle's front bumper was eventually forced over the top of the W-beam rail. The vehicle's tires climbed up the face of the W-Beam rail, causing the vehicle to vault over the bridge rail. The vehicle came to rest on the back side of the bridge rail, approximately 59 ft (18 m) downstream from impact, as shown in Figure 19. The vehicle's post-test trajectory is shown in Figure 14.

6.3 Vehicle Damage

Exterior vehicle damage was relatively minor and was limited to deformations of the steel frame, right-front quarter panel, and front bumper, as shown in Figure 20. The steel frame was

twisted due to the pickup vaulting over the bridge rail and impacting the ground behind the bridge rail. The right-side corner of the front bumper and the right-front quarter panel contained minor deformations, likely caused from the impact with the ground. No damage occurred to the interior occupant compartment. The vehicle damage was also assessed by the traffic accident scale (TAD) (23) and the vehicle damage index (SAE) (24), as shown in Figure 14.

6.4 Barrier Damage

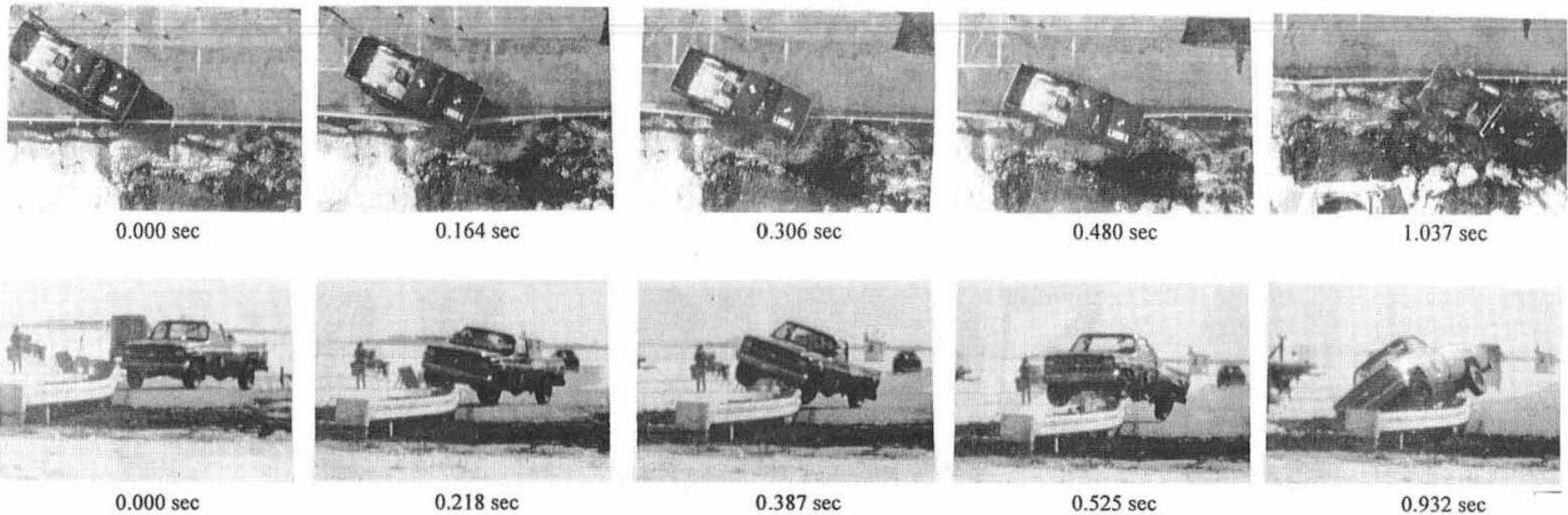
The minor damage to the bridge railing system is shown in Figures 21 through 23. Six timber posts were cracked or fractured. Plastic deformations to the connection angles and lag screws were also noticed. Contact marks, consisting of tire marks, gouges and indentations, and grease residue, were found along the length of the deformed W-beam rail. At post no. 7, the top of the W-beam rail pulled away from the top traffic-side face of the timber post. In addition, the washer, located under the head of the bolt and used to attach the rail to the post, had begun to pull through the slot. The maximum permanent set rail and post deflections were 14.3 in. (363 mm) and 13.8 in. (351 mm), respectively. No damage occurred to the timber bridge deck.

6.5 Occupant Risk Values

The normalized longitudinal and lateral occupant impact velocities were determined to be 8.7 ft/sec (2.6 m/sec) and 4.1 ft/sec (1.3 m/sec), respectively. The maximum 0.010-sec average occupant ridedown decelerations in the longitudinal and lateral directions were 18.6 g's and 7.5 g's, respectively. It is noted that the occupant impact velocities and occupant ridedown decelerations were within the suggested limits provided in NCHRP Report No. 350. The results of the occupant risk, determined from accelerometer data, are summarized in Figure 14. Results are shown graphically in Appendix A.



Figure 13. Impact Location, Test LVBR-1



Test Number	LVBR-1
Date	2/4/94
Total Installation Length	60.96 m
Bridge Rail Installation	Low-Volume Breakaway Bridge Rail
Bridge Rail Length	30.48 m
Steel W-Beam Rail	
Size	12 Gauge (2.66 mm)
Top Mounting Height	706 mm
Timber Bridge Posts (No. 1 through 15)	
Size (Dressed)	89 mm x 140 mm x 838 mm
Material	Dimension Lumber (CCA)
Grade	No. 2 or Better
Post-To-Deck Attachment Hardware	
Steel Angles (ASTM A36)	Two 9.5 mm x 127 mm x 127 mm
Post Anchor Bolts	Two 15.9-mm ϕ by 140-mm long
Lag Screws	Two 19.0-mm ϕ by 305-mm long
Timber Bridge Deck Installation	
Type	Longitudinal Glulam Deck Panels
Panel Size	273 mm x 1,219 mm x 5,715 mm
Material	West Coast Douglas Fir
Grade	Combination No. 2
Vehicle Model	1984 Chevrolet C-20 Pickup
Test Inertial Mass	2,041 kg
Gross Static Mass	2,041 kg

Vehicle Speed	
Impact	50.2 km/h
Exit	NA
Vehicle Angle	
Impact	26.8 degrees
Exit	NA
Vehicle Snagging	None
Vehicle Stability	Vehicle climbed and vaulted over the bridge rail
Effective Coefficient of Friction (μ)	NA
Occupant Impact Velocity - normalized	
Longitudinal	2.6 m/s (12 m/s) (1)
Lateral (not required)	1.3 m/s
Occupant Ridedown Deceleration - 0.010-sec average	
Longitudinal	18.6 g's (20 g's) (1)
Lateral (not required)	7.5 g's
Vehicle Damage	Minor
TAD ²³	1-RFQ-1
SAE ²⁴	01RFEW1
Maximum Vehicle Rebound Distance	NA
Bridge Rail Damage	Minor rail deformation and six fractured posts
Maximum Dynamic Deflection	NA
Maximum Permanent Set Deflection	363 mm

Figure 14. Summary of Test Results and Sequential Photographs, Test LVBR-1



0.000 sec



0.178 sec



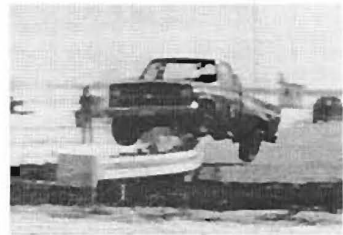
0.218 sec



0.297 sec



0.387 sec



0.525 sec



0.912 sec

Figure 15. Additional Sequential Photographs, Test LVBR-1



Figure 16. Documentary Photographs, Test LVBR-1



Figure 17. Documentary Photographs, Test LVBR-1



Figure 18. Documentary Photographs, Test LVBR-1



Figure 19. Vehicle Position at Rest, Test LVBR-1



Figure 20. Vehicle Damage, Test LVBR-1

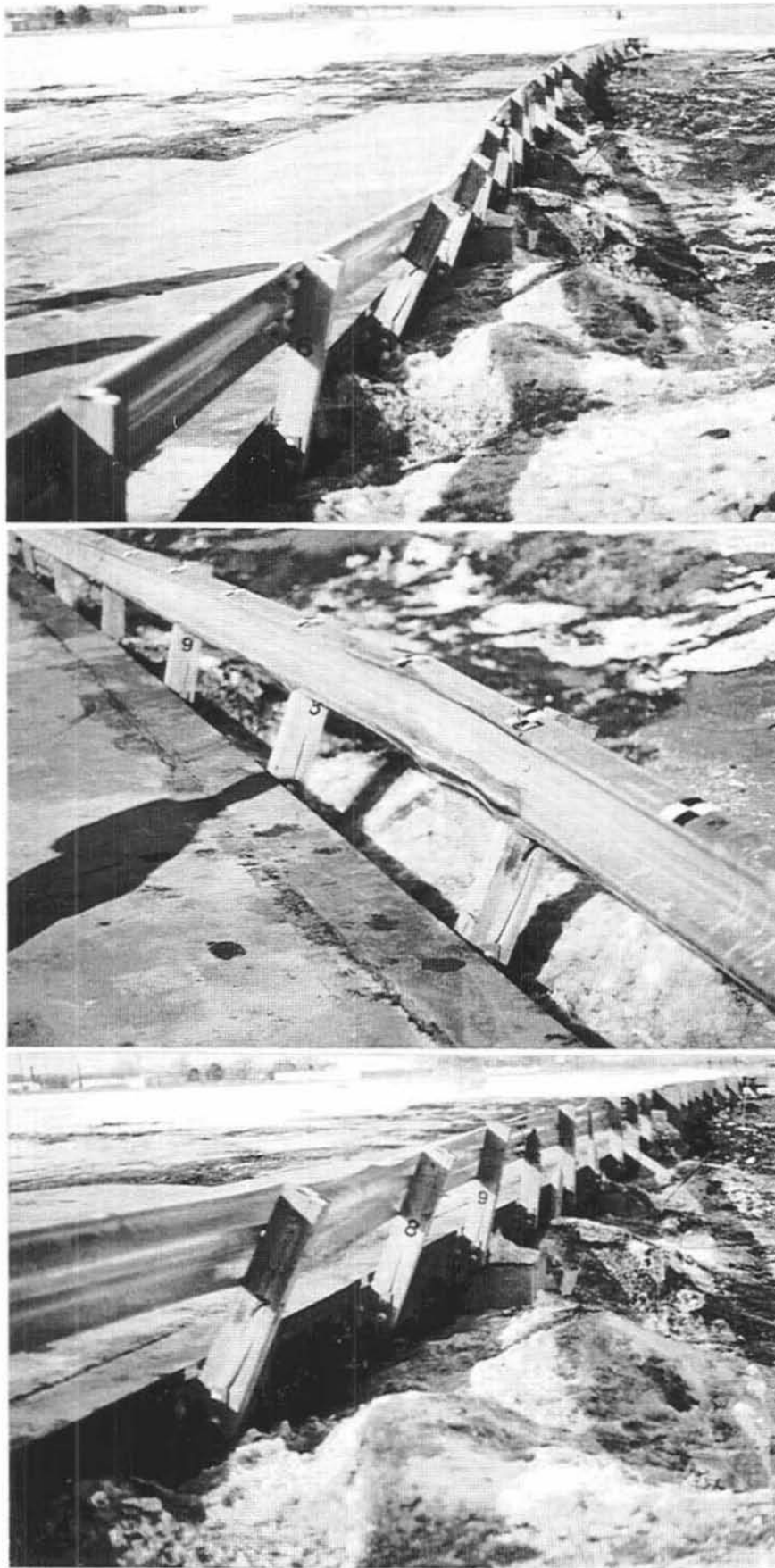


Figure 21. Bridge Rail Damage, Test LVBR-1



Figure 22. Bridge Post Damage, Test LVBR-1

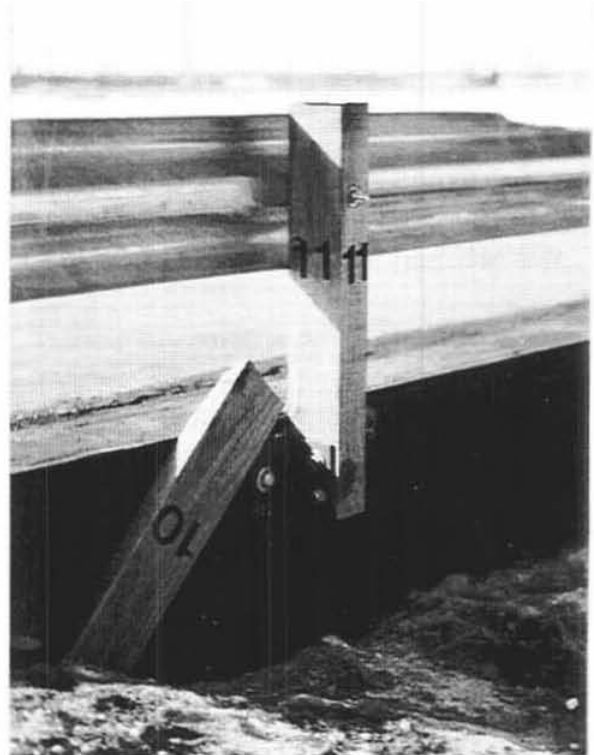
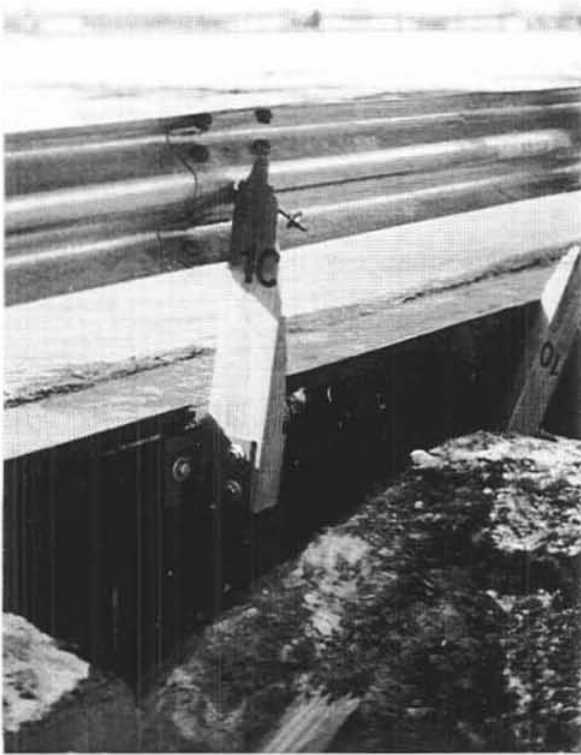


Figure 23. Bridge Post Damage, Test LVBR-1

7 TEST LVBR-1 DISCUSSION

Following test LVBR-1, a safety performance evaluation was conducted, and Design No. 1 was determined to be unacceptable according to the NCHRP Report No. 350 criteria. Therefore, it was necessary to determine the cause of the poor barrier performance so that design modifications could be made to the system.

A careful examination of the damaged barrier system and an analysis of the high-speed film revealed that the front bumper was not sufficiently captured between the two peaks of the W-beam rail. Thus, the bumper was allowed to extend over the top of the W-beam rail as the rail moved backward. Consequently, the right-front wheel climbed up the face of the W-beam rail, resulting in the vehicle vaulting over the top of the bridge railing. Failure of the bridge rail was directly attributed to insufficient rail mounting height. Therefore, the researchers believed that acceptable performance could be obtained by simply increasing the mounting height of the W-beam rail by lengthening the timber posts.

Originally, the post-to-deck attachment was designed so that little or no damage would occur to the timber deck or connection hardware. However, following test LVBR-1, plastic deformations were found in the connection angles and lag screws, probably as a result of the lateral loads imparted to the railing system. In order to minimize the deformations to the connection hardware, the concept of placing sawcuts in the timber posts was considered for weakening the posts to fracture or "breakaway" at a lower force level.

Therefore, additional static post tests were performed on several concepts to determine if the damage to the connection hardware could be minimized, and to develop the new force versus deflection relationship for a modified "breakaway" post concept.

8 RAIL SYSTEM DEVELOPMENT - PHASE II

8.1 Static Post Testing - Phase II

Twenty-four static tests, as summarized in Table 4, were performed on posts with increased post height and saw cuts in the compression zone, tension zone, and combinations thereof. Various sawcut configurations were placed in the posts to minimize deformations to the connection hardware. Typical damage to the timber post specimens is shown in Figure 24. A 4-in. by 6-in (102-mm by 152-mm) dimension lumber post measuring 36.75-in. (933-mm) long with steel angles measuring 5 in. by 5 in. by $\frac{3}{8}$ in. (127 mm by 127 mm by 10 mm) was selected for the modified design. The modified post chosen for Design No. 2 included a 1-in. (25-mm) horizontal saw cut placed on the tension side of the post, 3 in. (76 mm) from the base of the 36.75-in. (933-mm) long post. This sawcut configuration was chosen because it provided the best alternative for reducing the load imparted to the connection hardware while maintaining a reasonable level of structural capacity. The maximum static force for this post size and sawcut configuration was 1.15 kips (5.12 kN), as shown in Table 4. The length of the lumber post was increased from that used during Phase I to allow for an increase in the top mounting height of the W-beam rail.

8.2 Flexible W-Beam Bridge Railing System (Design No. 2)

In Design No. 2, the W-beam rail height was modified to the new metric standard of 21.65 in. (550 mm) as measured from the top of the asphalt surface to the center of the rail, thus providing a rail top mounting height of approximately 27.78 in. (706 mm). The flat washer located under the head of the W-Beam bolt was removed to allow for the rail to release more easily from the lumber post and not be pulled downward. Photographs of the modified bridge railing system are shown in Figure 25. Detailed drawings of the modified bridge rail components are provided in Figure 26.

Table 4. Static Post Testing Results - Phase II

Test No.	Hardware Sizes		Bolt Torque (ft-lbs)	Peak Load (lbs)	Deflection @ Peak Load (in.)
	Timber Post	Steel Angles			
LVRRT-11	4 x 6	5 x 5 x 3/8	75	1500	7.5
LVRPT-12	4 x 6	5 x 5 x 3/8	75	1600	8.8
LVRPT-13 ¹	4 x 6	5 x 5 x 3/8	75	2000	10.9
LVRPT-14 ^U	4 x 6	5 x 5 x 3/8	75	1750	9.1
LVRPT-15 ²	4 x 6	5 x 5 x 3/8	75	1875	12.1
LVRPT-16 ²	4 x 6	5 x 5 x 3/8	75	1750	7.3
LVRPT-17 ³	4 x 6	5 x 5 x 3/8	75	2125	13.3
LVRPT-18 ⁴	4 x 6	5 x 5 x 3/8	75	1875	10.9
LVRPT-19 ⁵	4 x 6	5 x 5 x 3/8	75	1875	10.4
LVRPT-20 ⁵	4 x 6	5 x 5 x 3/8	75	1875	9.7
LVRPT-21 ⁴	4 x 6	5 x 5 x 3/8	75	1750	8.6
LVRPT-22 ⁴	4 x 6	5 x 5 x 3/8	75	1675	9.4
LVRPT-23 ⁶	4 x 6	5 x 5 x 3/8	75	1875	12.3
LVRPT-24 ⁶	4 x 6	5 x 5 x 3/8	75	1625	14.2
LVRPT-25 ⁷	4 x 6	5 x 5 x 3/8	75	1625	13.6
LVRPT-26 ⁷	4 x 6	5 x 5 x 3/8	75	1200	10.9
LVRPT-27 ⁴	4 x 6	5 x 5 x 3/8	75	1750	10.9
LVRPT-28 ⁸	4 x 6	5 x 5 x 3/8	75	1625	13.9
LVRPT-29 ⁹	4 x 6	5 x 5 x 3/8	75	1150	9.1
LVRPT-30	4 x 6	5 x 5 x 3/8	75	2125	13.7
LVRPT-31 ¹⁰	4 x 6	5 x 5 x 3/8	75	250	1.0
LVRPT-32 ¹¹	4 x 6	5 x 5 x 3/8	75	625	3.3
LVRPT-33 ¹²	4 x 6	5 x 5 x 3/8	75	875	5.4
LVRPT-34 ¹³	4 x 6	5 x 5 x 3/8	75	1625	11.6

- ¹ - ½-in. cut in compression zone.
- ² - 1-in. cut in compression zone.
- ³ - 1½-in. cut in compression zone.
- ⁴ - 1½-in. cut in compression zone with steel wedge plate.
- ⁵ - 2-in. cut in compression zone with steel wedge plate.
- ⁶ - 2-in. cut in compression zone with steel wedge plate and ½-in. cut in tension zone.
- ⁷ - 2-in. cut in compression zone with steel wedge plate and 1-in. cut in tension zone.
- ⁸ - 1½-in. cut in compression zone with steel wedge plate and 1-in. cut in tension zone.
- ⁹ - 1-in. cut in tension zone.
- ¹⁰ - 3½-in. cut in tension zone.
- ¹¹ - 2-in. cut in tension zone.
- ¹² - 1½-in. cut in tension zone.
- ¹³ - ½-in. cut in tension zone.
- ^U - Unknown cut information

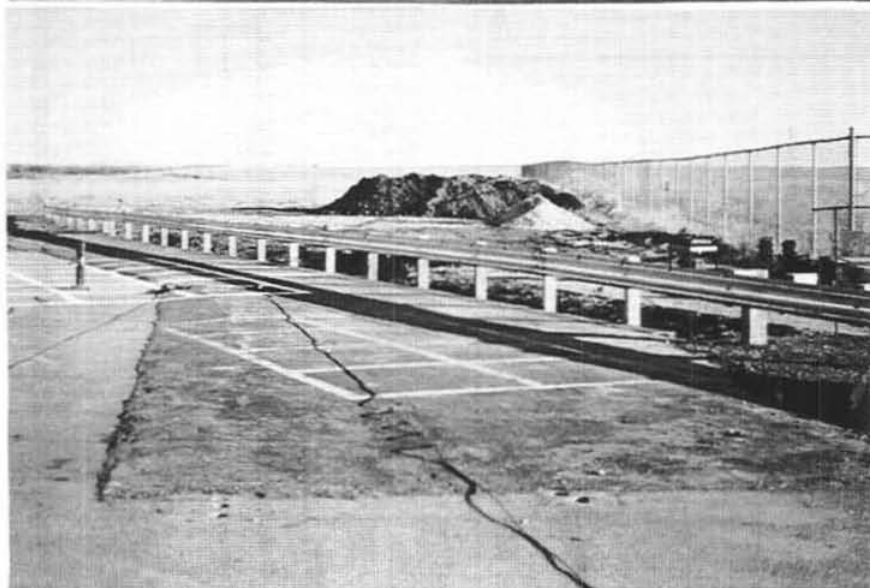
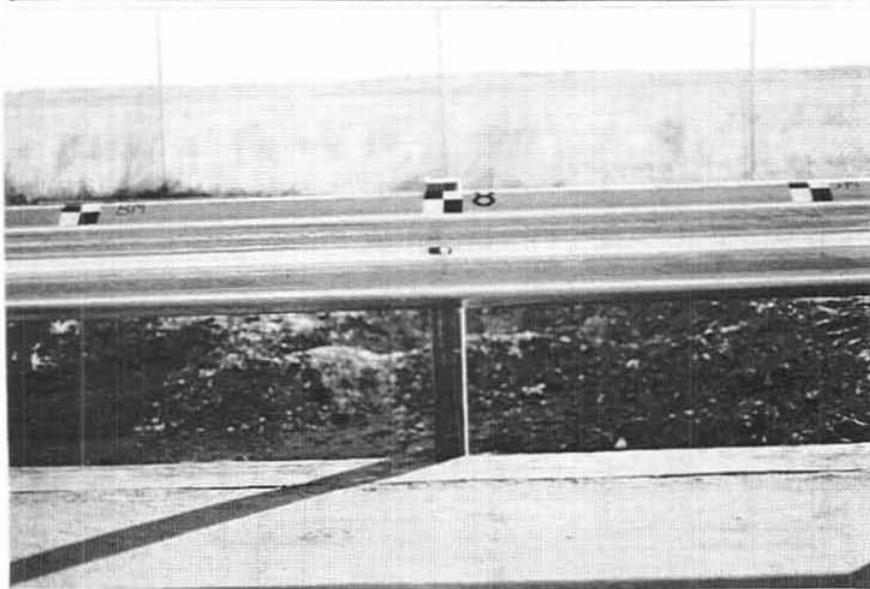
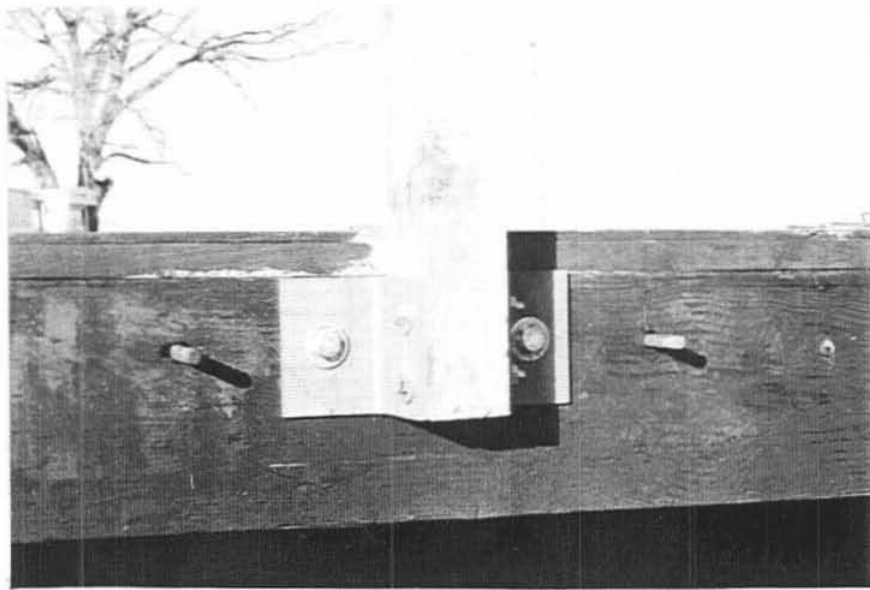


Figure 25. W-Beam Bridge Railing, Design No. 2

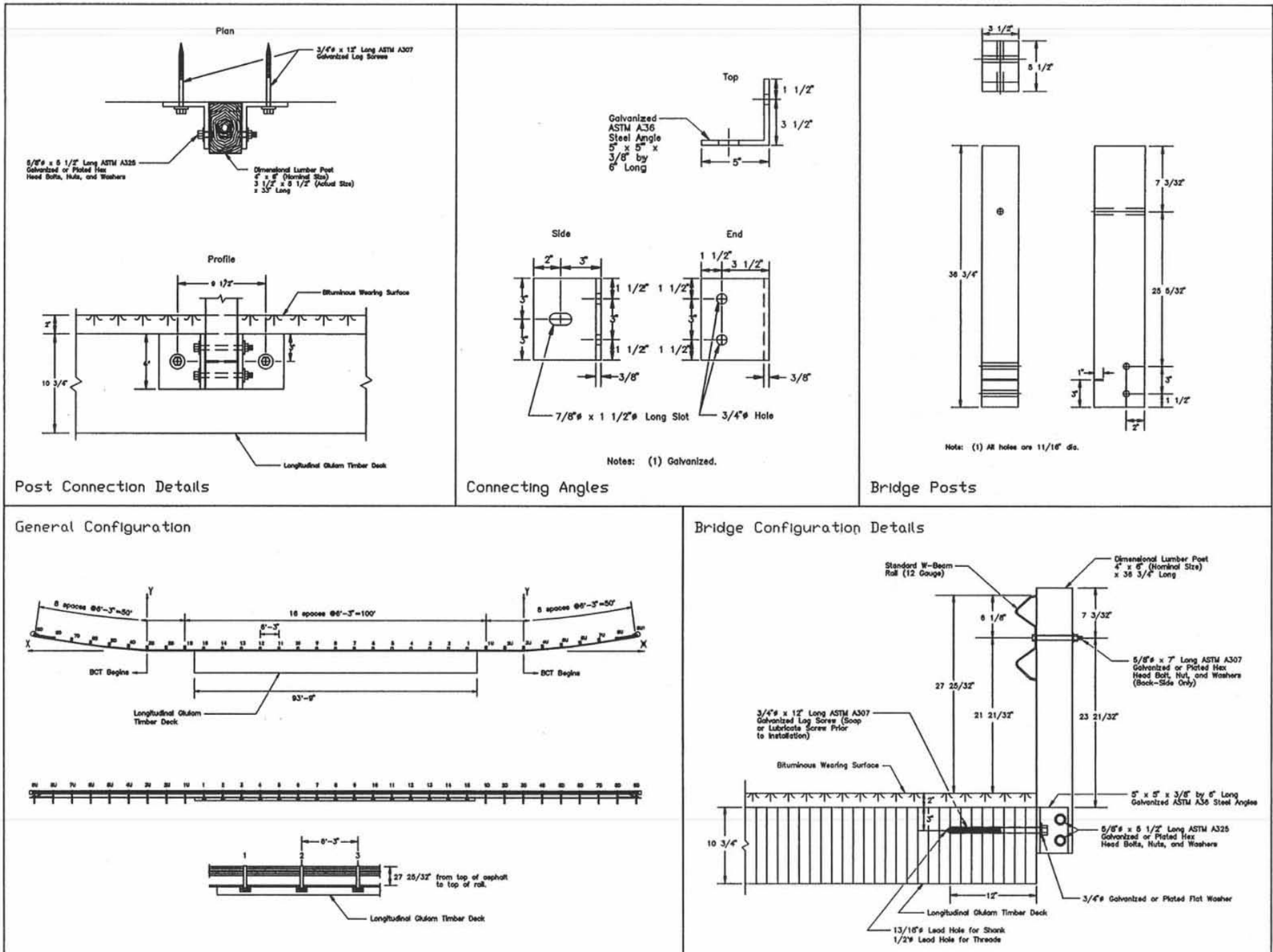


Figure 26. Flexible W-Beam Bridge Railing System Design Details, Design No. 2

8.3 Computer Simulation Modeling - Phase II

BARRIER VII simulation modeling was performed on Design No. 2 to analyze the dynamic performance of the bridge railing. Computer simulation was conducted with a 1,996-kg (4,400-lb) pickup truck impacting at 31 mph (50 km/h) and 25 degrees according to TL-1 of NCHRP Report No. 350.

The simulation results indicated that the flexible bridge railing design satisfactorily redirected the 1,996-kg (4,400-lb) pickup truck. For Design No. 2, computer simulation predicted that eight timber posts would be broken during impact, and the maximum dynamic deflection of the W-Beam was predicted to be 32.5 in. (825 mm). In addition, the predicted peak 0.050-sec average impact force perpendicular to the bridge railing was approximately 6.0 kips (26.7 kN).

9 FULL-SCALE CRASH TEST - DESIGN NO. 2

9.1 Test LVBR-2 (4,504 lbs (2,043 kg), 30.6 mph (49.2 km/hr), 24.9 degrees)

A 1985 Chevrolet C-20 pickup truck impacted the W-beam bridge railing at post no. 7, as shown in Figure 27. A summary of the test results and the sequential photographs is presented in Figure 28. Additional sequential photographs are shown in Figure 29. Documentary photographs of the crash test are shown in Figures 30 through 31.

9.2 Test Description

Following the initial impact with the bridge rail, the W-beam rail began to deflect laterally as several timber posts began to fracture. At 0.158 sec after impact, the right-front corner of the vehicle was near post no. 8. As the W-beam continued to deflect laterally, the vehicle contact caused the W-beam rail to rotate and move downward. At 0.316 and 0.474 sec after impact, the right-front corner of the vehicle was near post no. 9 and 10, respectively. The vehicle became parallel to the bridge railing at 0.652 sec with a velocity of 24.1 mph (38.8 km/h). From the overhead high-speed film, the maximum dynamic lateral deflection was 51.9 in. (1,318 mm) at the midspan between post nos. 9 and 10 at 0.890 sec. Although the vehicle was redirected, it did not exit the bridge railing. The vehicle came to rest 44 ft (13.4 m) downstream from impact with the vehicle's left-side tires and right-side undercarriage resting on the deck surface, as shown in Figure 32. It is noted that at no time, during impact or any time thereafter, did the vehicle's right-side tires contact the ground. The vehicle's post-test trajectory is shown in Figure 28.

9.3 Vehicle Damage

Exterior vehicle damage was minor. Damage was evident on the right-front quarter panel due to vehicle-rail contact and the right-side undercarriage due to contact with the outer top surface of

the deck, as shown in Figure 33. No damage occurred to the interior occupant compartment. Following the crash test, the vehicle's right-side tires were lifted onto the deck, and the vehicle was driven away. The vehicle damage was also assessed by the traffic accident scale (TAD) (23) and the vehicle damage index (SAE) (24), as shown in Figure 28.

9.4 Barrier Damage

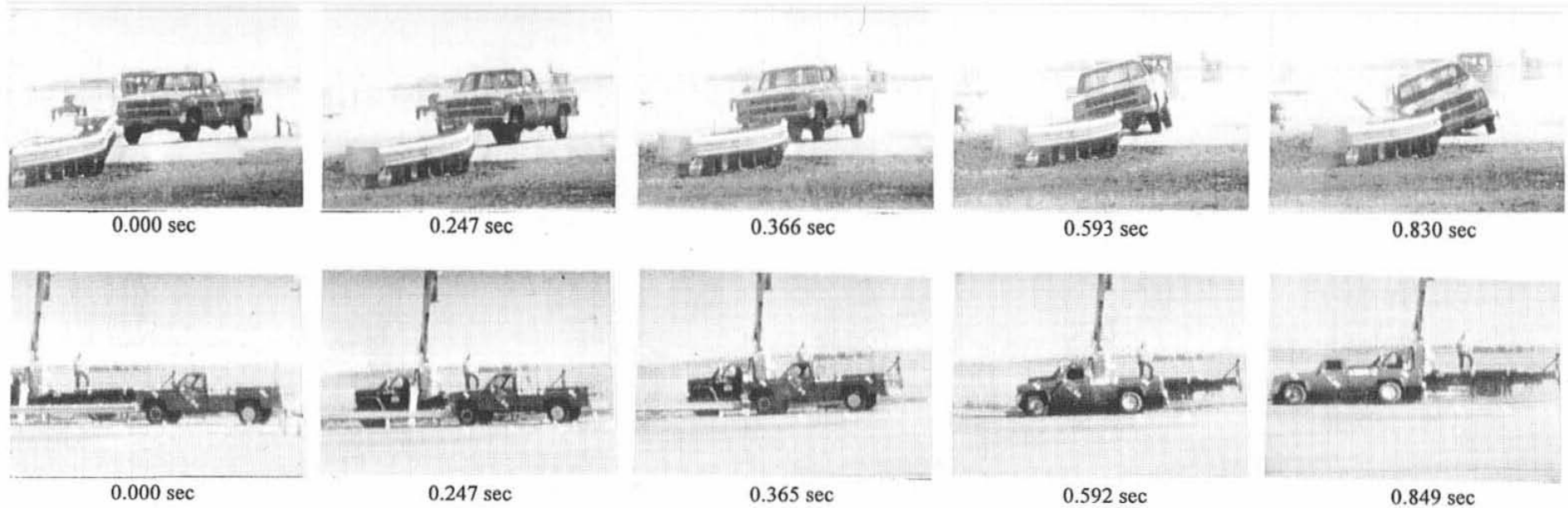
The moderate damage to the bridge railing system is shown in Figure 34, as well as in photographs provided in Figures 32 through 33. One 6-ft 3-in. (1.90-m) section of W-Beam rail was permanently damaged. Eleven posts, post nos. 4 through 14 fractured away from the deck attachment. In addition, five steel angles were deformed downstream of impact due to contact between the angles and the undercarriage of the vehicle. The timber deck surface near the edge was also scraped due contact from the vehicle undercarriage. The maximum permanent set and dynamic rail deflections were 45.4 in. (1,153 mm) and 51.9 in. (1,318 mm), respectively. No damage occurred to the timber bridge deck.

9.5 Occupant Risk Values

The normalized longitudinal and lateral occupant impact velocities were determined to be 7.4 ft/sec (2.2 m/sec) and 6.3 ft/sec (1.9 m/sec), respectively. The maximum 0.010-sec average occupant ridedown decelerations in the longitudinal and lateral directions were 4.3 g's and 3.8 g's, respectively. It is noted that the occupant impact velocities and occupant ridedown decelerations were within the suggested limits provided in NCHRP Report No. 350. The results of the occupant risk, determined from accelerometer data, are summarized in Figure 28. Results are shown graphically in Appendix A.



Figure 27. Impact Location, Test LVBR-2

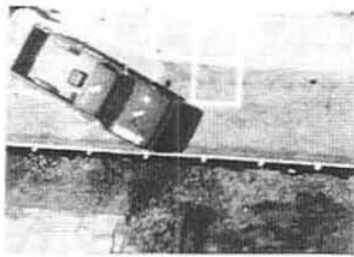


57

Test Number	LVBR-2
Date	3/18/94
Total Installation Length	60.96 m
Bridge Rail Installation	Low-Volume Breakaway Bridge Rail
Bridge Rail Length	30.48 m
Steel W-Beam Rail	
Size	12 Gauge (2.66 mm)
Top Mounting Height	706 mm
Timber Bridge Posts (No. 1 through 15)	
Size (Dressed)	89 mm x 140 mm x 933 mm
Material	Dimension Lumber (CCA)
Grade	No. 2 or Better
Post-To-Deck Attachment Hardware	
Steel Angles (ASTM A36)	Two 9.5 mm x 127 mm x 127 mm
Post Anchor Bolts	Two 15.9-mm ϕ by 140-mm long
Lag Screws	Two 19.0-mm ϕ by 305-mm long
Timber Bridge Deck Installation	
Type	Longitudinal Glulam Deck Panels
Panel Size	273 mm x 1,219 mm x 5,715 mm
Material	West Coast Douglas Fir
Grade	Combination No. 2
Vehicle Model	1985 Chevrolet C-20 Pickup
Test Inertial Mass	2,043 kg
Gross Static Mass	2,043 kg

Vehicle Speed	
Impact	49.2 km/h
Exit	NA
Vehicle Angle	
Impact	24.9 degrees
Exit	NA
Vehicle Snagging	None
Vehicle Stability	Satisfactory
Effective Coefficient of Friction (μ)	0.28 (Fair)
Occupant Impact Velocity - normalized	
Longitudinal	2.2 m/s (12 m/s) (L)
Lateral (not required)	1.9 m/s
Occupant Ridedown Deceleration - 0.010-sec average	
Longitudinal	4.3 g's (20 g's) (L)
Lateral (not required)	3.8 g's
Vehicle Damage	Minor
TAD ²³	I-RFQ-1
SAE ²⁴	01RFEW1
Maximum Vehicle Rebound Distance	NA
Bridge Rail Damage	Minor rail deformation and eleven fractured posts
Maximum Dynamic Deflection	131.8 cm
Maximum Permanent Set Deflection	115.3 cm

Figure 28. Summary of Test Results and Sequential Photographs, Test LVBR-2



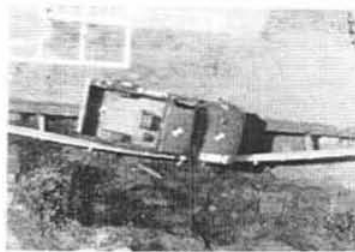
0.000 sec



0.158 sec



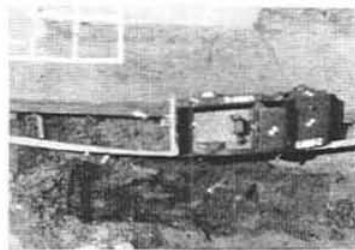
0.316 sec



0.544 sec



0.652 sec



0.899 sec



0.000 sec



0.151 sec



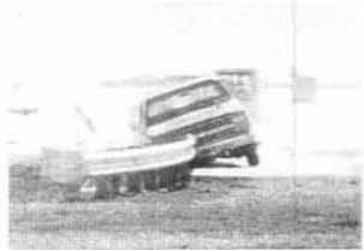
0.321 sec



0.552 sec



0.663 sec



0.914 sec

Figure 29. Additional Sequential Photographs, Test LVBR-2



Figure 30. Documentary Photographs, Test LVBR-2



Figure 31. Documentary Photographs, Test LVBR-2



Figure 32. Vehicle Position at Rest, Test LVBR-2



Figure 33. Vehicle Damage, Test LVBR-2

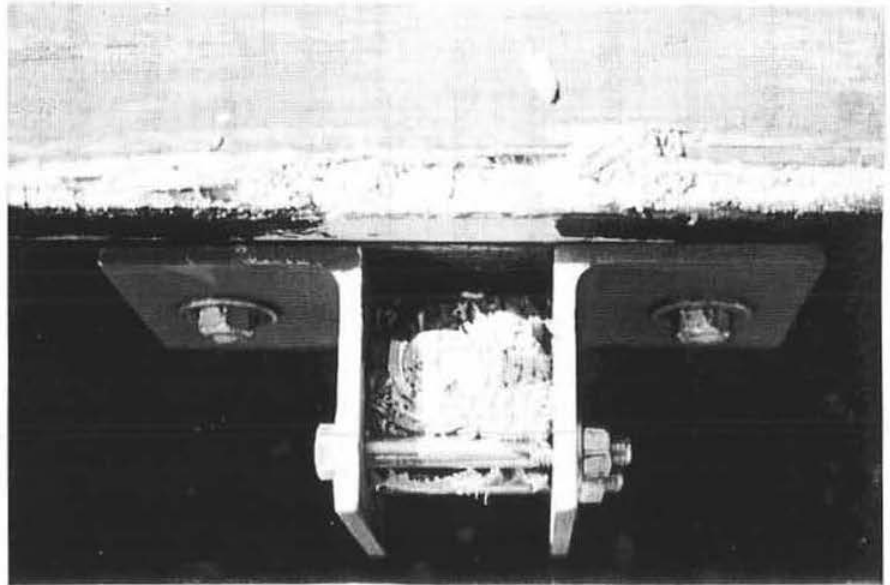
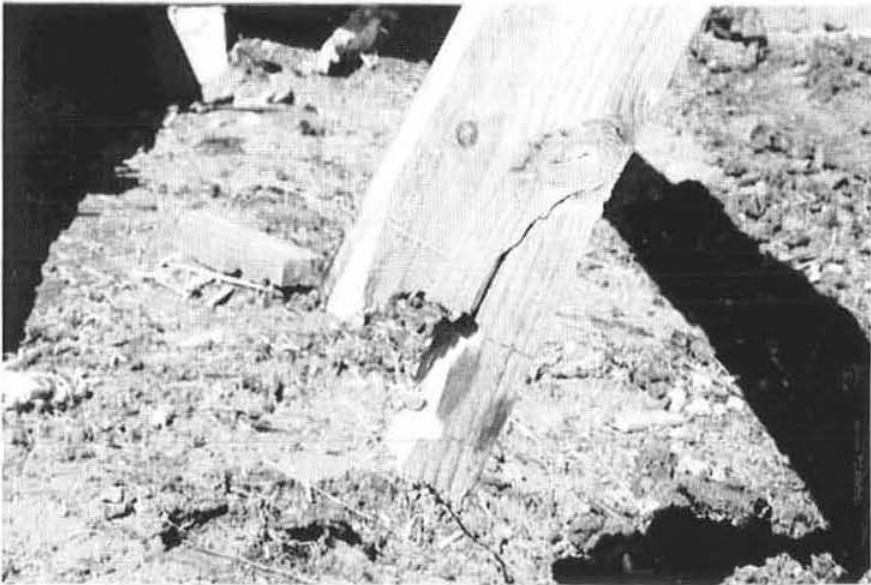


Figure 34. Typical Bridge Rail and Post Damage, Test LVBR-2

10 TEST LVBR-2 DISCUSSION

Following test LVBR-2, a safety performance evaluation was conducted, and Design No. 2 was determined to be acceptable according to the NCHRP Report No. 350 criteria. The modified breakaway bridge rail contained and redirected the test vehicle without penetration or overriding of the barrier. Detached elements, fragments, or other debris from the bridge rail did not penetrate or show potential for penetrating the occupant compartment, and would not present any hazard to other traffic or pedestrians. The integrity of the occupant compartment was maintained with no intrusion or deformation. The vehicle remained upright during and after collision, and the vehicle's trajectory did not intrude into adjacent traffic lanes. Thus, the modified breakaway bridge railing successfully met all the evaluation criteria for Test Level 1 of NCHRP Report No. 350. A summary of the safety performance evaluation for tests LVBR-1 and LVBR-2 are provided in Table 5.

Table 5. Summary of Safety Performance Evaluation

Evaluation Factors	Evaluation Criteria	Test LVBR-1	Test LVBR-2
Structural Adequacy	A. Test article should contain and redirect the vehicle; the vehicle should not penetrate, underride, or override the installation although controlled lateral deflection of the test article is acceptable.	U	S
Occupant Risk	D. Detached elements, fragments or other debris from the test article should not penetrate or show potential for penetrating the occupant compartment, or present an undue hazard to other traffic, pedestrians, or personnel in a work zone. Deformations of, or intrusions into, the occupant compartment that could cause serious injuries should not be permitted.	S	S
	F. The vehicle should remain upright during and after collision although moderate roll, pitching and yawing are acceptable.	S	S
Vehicle Trajectory	K. After collision it is preferable that the vehicle's trajectory not intrude into adjacent traffic lanes.	S	S
	L. The occupant impact velocity in the longitudinal direction should not exceed 12 m/sec and the occupant ridedown acceleration in the longitudinal direction should not exceed 20 G's.	S	S
	M. The exit angle from the test article preferably should be less than 60 percent of test impact angle, measured at time of vehicle loss of contact with test device.	S	S

S - (Satisfactory)
 U - (Unsatisfactory)

11 CONCLUSIONS

A flexible railing with a "breakaway" post system was developed and full-scale crash tested for use on longitudinal glulam timber decks with low traffic volumes and speeds. Two crash tests were performed according to Test Level 1 (TL-1) of NCHRP Report No. 350. The first crash test, test LVBR-1, failed after the vehicle vaulted over the bridge railing due to insufficient rail height. Following this crash test, the bridge railing system was modified by increasing the top mounting height of the W-beam rail to 27.78 in. (706 mm), providing a 1-in. (25-mm) sawcut in the tension zone of the base of the timber posts, and removing the washer located between the head of the post bolt and the face of the W-beam rail. A retest, test LVBR-2, was performed on the modified system and was determined to be acceptable according to the TL-1 crash test conditions of NCHRP Report No. 350.

The side-mounted railing system provides an economic railing with readily available materials. Material costs for the bridge railing system were reasonably low at approximately \$7.88/ft (\$25.85/m). In addition, the W-beam bridge railing system was easy to install and should have low construction labor costs. This railing system should also be adaptable to other types of longitudinal timber decks with little or no modification. In addition, damage to the bridge deck was limited to minor scrapes, therefore repair costs would also be kept to an absolute minimum.

Therefore, the successful completion of this research project resulted in a W-beam bridge railing having acceptable safety performance and meeting current crash test safety standards.

12 RECOMMENDATIONS

The low-cost, flexible W-beam bridge railing with "breakaway" posts described herein was successfully developed for low impact condition requirements. For flexible railings with "breakaway" posts, the full-scale crash testing program indicates that acceptable impact performance is possible although large dynamic rail deflections can be expected. Due to the magnitude of the dynamic deflections observed during test LVBR-2, it is recommended that the bridge railing system described herein be limited to applications where the railing length is less than or equal to the crash tested length.

Similar flexible railings, with a modified post-to-deck attachment and stronger posts, may be capable of meeting the performance requirements of Test Level 2 from NCHRP Report No. 350. However, any design modifications made to the bridge railing system can only be verified through the use of full-scale vehicle crash testing. Thus, it is recommended that the research described herein be extended to develop higher performance flexible railings for timber bridge decks.

13 REFERENCES

1. Ross, H.E., Sicking, D.L., Zimmer, R.A. and Michie, J.D., *Recommended Procedures for the Safety Performance Evaluation of Highway Features*, National Cooperative Highway Research Program (NCHRP) Report No. 350, Transportation Research Board, Washington, D.C., 1993.
2. *Guide Specifications for Bridge Railings*, American Association of State Highway and Transportation Officials, Washington, D.C., 1989.
3. Faller, R.K., Ritter, M.A., Holloway, J.C., Pfeifer, B.G., and B.T. Rosson, *Performance Level 1 Bridge Railings for Timber Decks*, Transportation Research Record No. 1419, Transportation Research Board, National Research Council, Washington D.C., 1993.
4. Ritter, M.A., Lee, P.D.H., Faller, R.K., Rosson, B.T., and S.R. Duwaldi, *Plans for Crash Tested Bridge Railings for Longitudinal Wood Decks*, General Technical Report No. FPL-GTR-87, United States Department of Agriculture, Forest Service, Forest Products Laboratory, Madison, Wisconsin, September 1995.
5. Ritter, M.A. and R.K. Faller, *Crashworthy Bridge Railings for Longitudinal Wood Decks*, Paper presented by Ritter at the 1994 Pacific Timber Engineering Conference, Gold Coast, Australia, July 11-15, 1994.
6. Ritter, M.A., Faller, R.K., and Duwaldi, S.R., *Crash-Tested Bridge Railings for Timber Bridges*, Presented by Ritter at the Fourth International Bridge Engineering Conference, Volume 2, Conference Proceedings 7, San Francisco, California, August 28-30, 1995, Transportation Research Board, Washington, D.C.
7. Rosson, B.T., Faller, R.K., and M.A. Ritter, *Performance Level 2 and Test Level 4 Bridge Railings for Timber Decks*, Transportation Research Record No. 1500, Transportation Research Board, National Research Council, Washington D.C., 1995.
8. Faller, R.K., Rosson, B.T., Ritter, M.A., and Sicking, D.L., *Design and Evaluation of Two Low-Volume Bridge Railings*, Presented at the Sixth International Conference on Low-Volume Roads, Volume 2, Conference Proceedings 6, University of Minnesota, Minneapolis, Minnesota, June 25-29, 1995, Transportation Research Board, Washington, D.C.
9. Hancock, K.L., Hansen, A.G. and J.B. Mayer, *Aesthetic Bridge Rails, Transitions, and Terminals for Park Roads and Parkways*, Report No. FHWA-RD-90-052, Submitted to the Office of Safety and Traffic Operations R&D, Federal Highway Administration, Performed by the Scientex Corporation, May 1990.

10. Raju, P.R., GangaRao, H.V.S., Mak, K.K. and D.C. Alberson, *Timber Bridge Rail Testing and Evaluation: Timber Bridge Rail, Posts, and Deck on Steel Stringers*, Final Report, Volume 1, Constructed Facilities Center, West Virginia University, Morgantown, WV, October 1993.
11. Raju, P.R., GangaRao, H.V.S., Mak, K.K. and D.C. Alberson, *Timber Bridge Rail and Transition Rail Testing and Evaluation: Glulam Bridge Rail and Deck on Glulam Stringers*, Final Report, Volume 2, Constructed Facilities Center, West Virginia University, Morgantown, WV, October 1993.
12. Raju, P.R., GangaRao, H.V.S., Mak, K.K. and D.C. Alberson, *Timber Bridge Rail and Transition Rail Testing and Evaluation: W-Beam Steel Rail, Timber Posts and Glulam Deck on Steel Stringers*, Final Report, Volume 3, Constructed Facilities Center, West Virginia University, Morgantown, WV, October 1993.
13. Raju, P.R., GangaRao, H.V.S., Duwaldi, S.R. and H.K. Thippeswamy, *Development and Testing of Timber Bridge and Transition Rails for Transverse Glued-Laminated Bridge Decks*, Transportation Research Record No. 1460, Transportation Research Board, National Research Council, Washington D.C., 1994.
14. Stoughton, R.L., Stoker, J.R., Nagai, I., Hale, P., Jr., and Bishop, R.W., *Vehicle Impact Tests of a See-Through, Collapsing Ring, Structural Steel Tube, Bridge Barrier Railing*, Report No. FHWA/CA/TL-83/05, Office of Transportation Laboratory, California Department of Transportation, June 1983.
15. Hirsch, T.J., Panak, J.J., and Buth, C.E., *Tubular W-Beam Bridge Rail*, Report No. FHWA/TX78-230-1 or TTI-2-5-78-230-1, Submitted to Texas State Department of Highways and Public Transportation, Performed by Texas Transportation Institute, Texas A&M University, October 1978.
16. Bronstad, M.E., and Michie, J.D., *Multiple-Service-Level Highway Bridge Railing Selection Procedures*, National Cooperative Highway Research Program (NCHRP) Report No. 239, Transportation Research Board, National Research Council, Washington, D.C., November 1981.
17. Buth, C.E., Campise, W.L., Griffin III, L.I., Love, M.L., and Sicking, D.L., *Performance Limits of Longitudinal Barrier Systems - Volume I: Summary Report*, FHWA/RD-86/153, Final Report to the Federal Highway Administration, Office of Safety and Traffic Operations R&D, Performed by Texas Transportation Institute, Texas A&M University, May 1986.
18. Ross, H.E., Jr., Perera, H.S., Sicking, D.L., and Bligh, R.P., *Roadside Safety Design for Small Vehicles*, National Cooperative Highway Research Program (NCHRP) Report No. 318, Transportation Research Board, Washington, D.C., May 1989.

19. *American Wood-Preservers' Association Book of Standards*, American Wood-Preservers' Association, Woodstock, Md., 1991.
20. Powell, G.H., *BARRIER VII: A Computer Program For Evaluation Of Automobile Barrier Systems*, Prepared for: Federal Highway Administration, Report No. FHWA RD-73-51, April 1973.
21. Hinch, J., Yang, T-L, and Owings, R., *Guidance Systems for Vehicle Testing*, ENSCO, Inc., Springfield, VA, 1986.
22. Taborck, J.J., "Mechanics of Vehicles - 7", *Machine Design Journal*, May 30, 1957.
23. *Vehicle Damage Scale for Traffic Investigators*, Second Edition, Technical Bulletin No. 1, Traffic Accident Data (TAD) Project, National Safety Council, Chicago, Illinois, 1971.
24. *Collision Deformation Classification - Recommended Practice J224 March 1980*, Handbook Volume 4, Society of Automotive Engineers (SAE), Warrendale, Pennsylvania, 1985.

14 APPENDICES

APPENDIX A - ACCELEROMETER DATA ANALYSIS

Figure A-1. Graph of Longitudinal Deceleration, Test LVBR-1

Figure A-2. Graph of Longitudinal Occupant Impact Velocity, Test LVBR-1

Figure A-3. Graph of Longitudinal Occupant Displacement, Test LVBR-1

Figure A-4. Graph of Lateral Deceleration, Test LVBR-1

Figure A-5. Graph of Lateral Occupant Impact Velocity, Test LVBR-1

Figure A-6. Graph of Lateral Occupant Displacement, Test LVBR-1

Figure A-7. Graph of Longitudinal Deceleration, Test LVBR-2

Figure A-8. Graph of Longitudinal Occupant Impact Velocity, Test LVBR-2

Figure A-9. Graph of Longitudinal Occupant Displacement, Test LVBR-2

Figure A-10. Graph of Lateral Deceleration, Test LVBR-2

Figure A-11. Graph of Lateral Occupant Impact Velocity, Test LVBR-2

Figure A-12. Graph of Lateral Occupant Displacement, Test LVBR-2

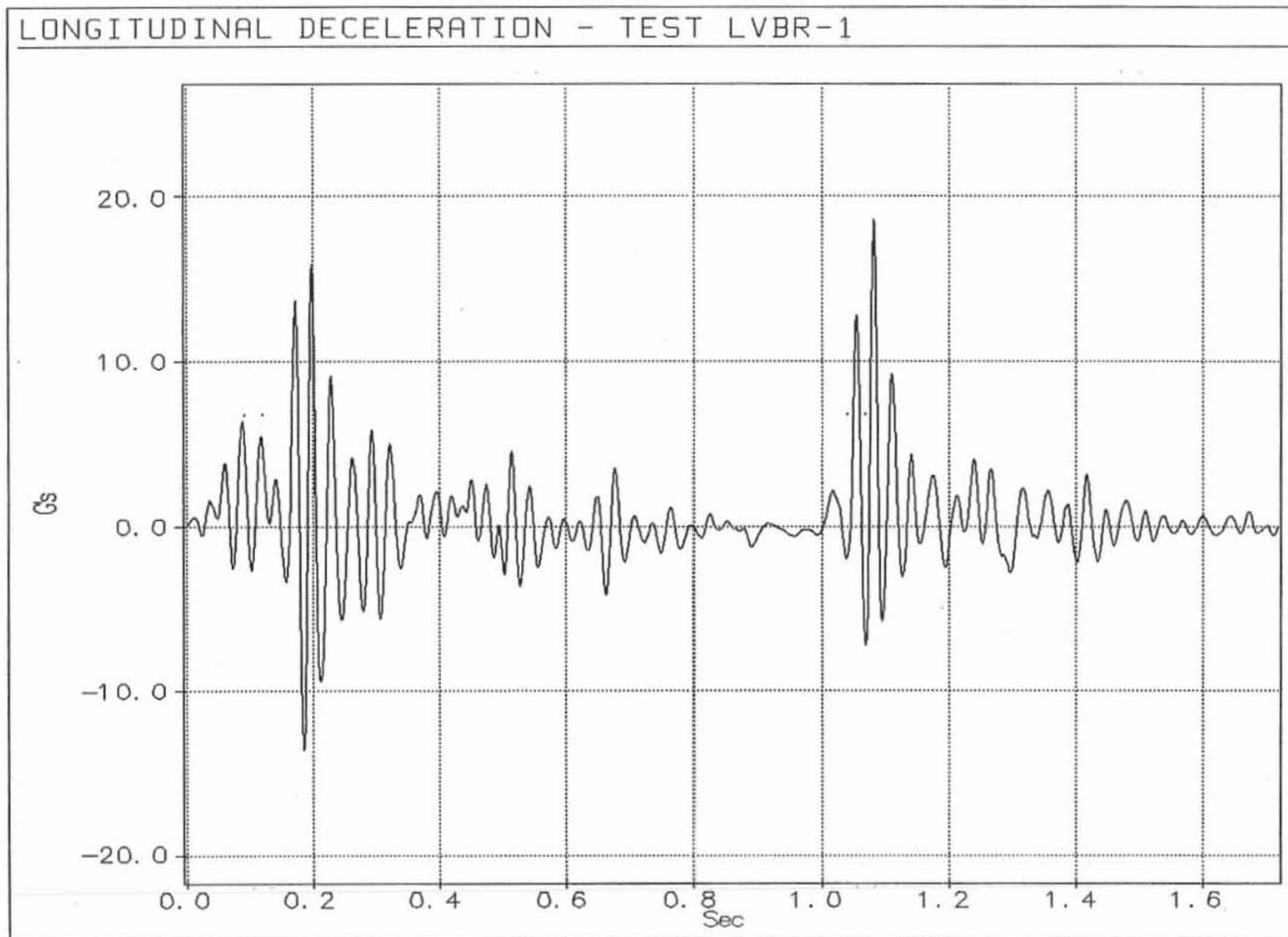


Figure A-1. Graph of Longitudinal Deceleration, Test LVBR-1



Figure A-2. Graph of Longitudinal Occupant Impact Velocity, Test LVBR-1

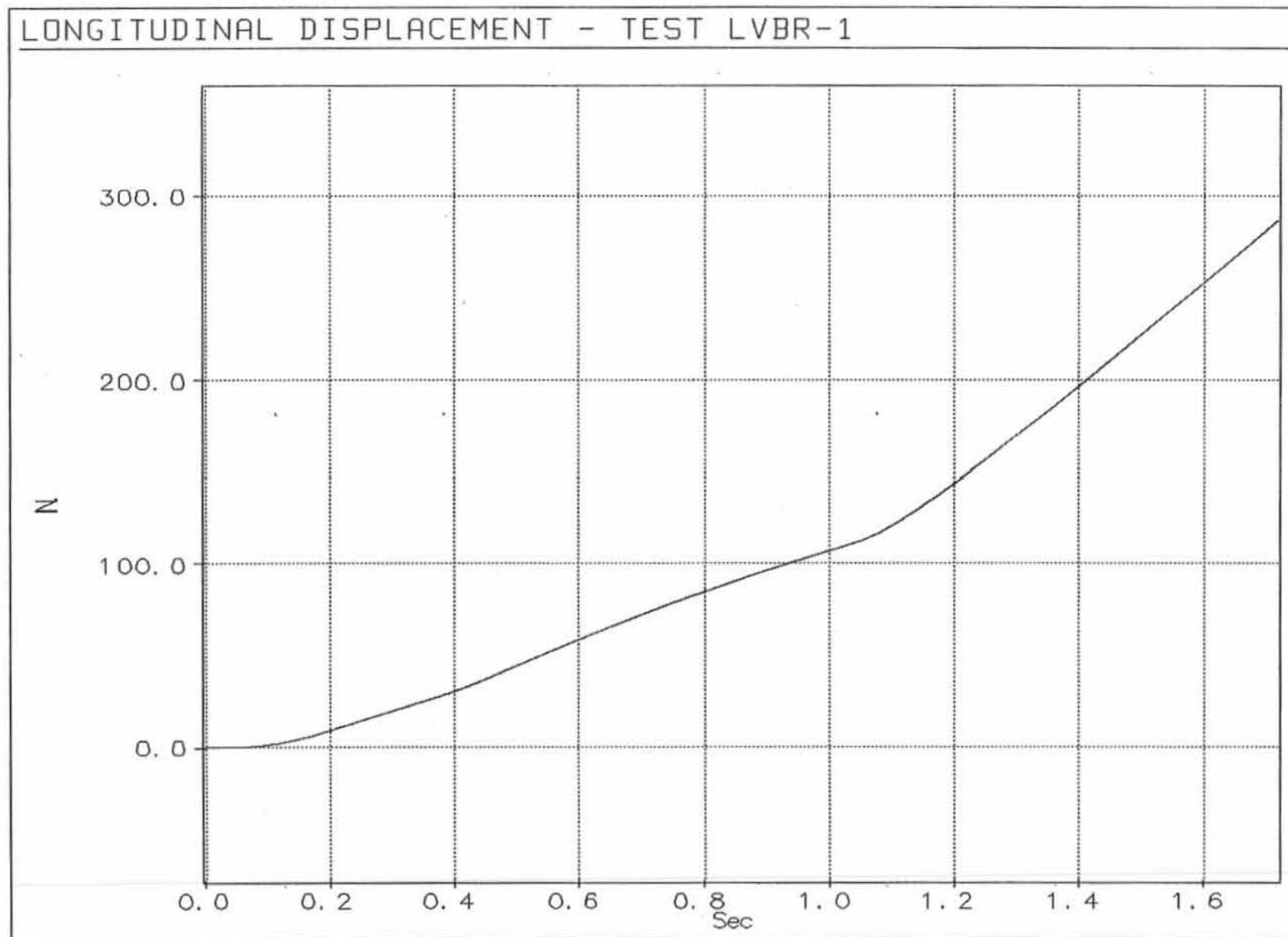
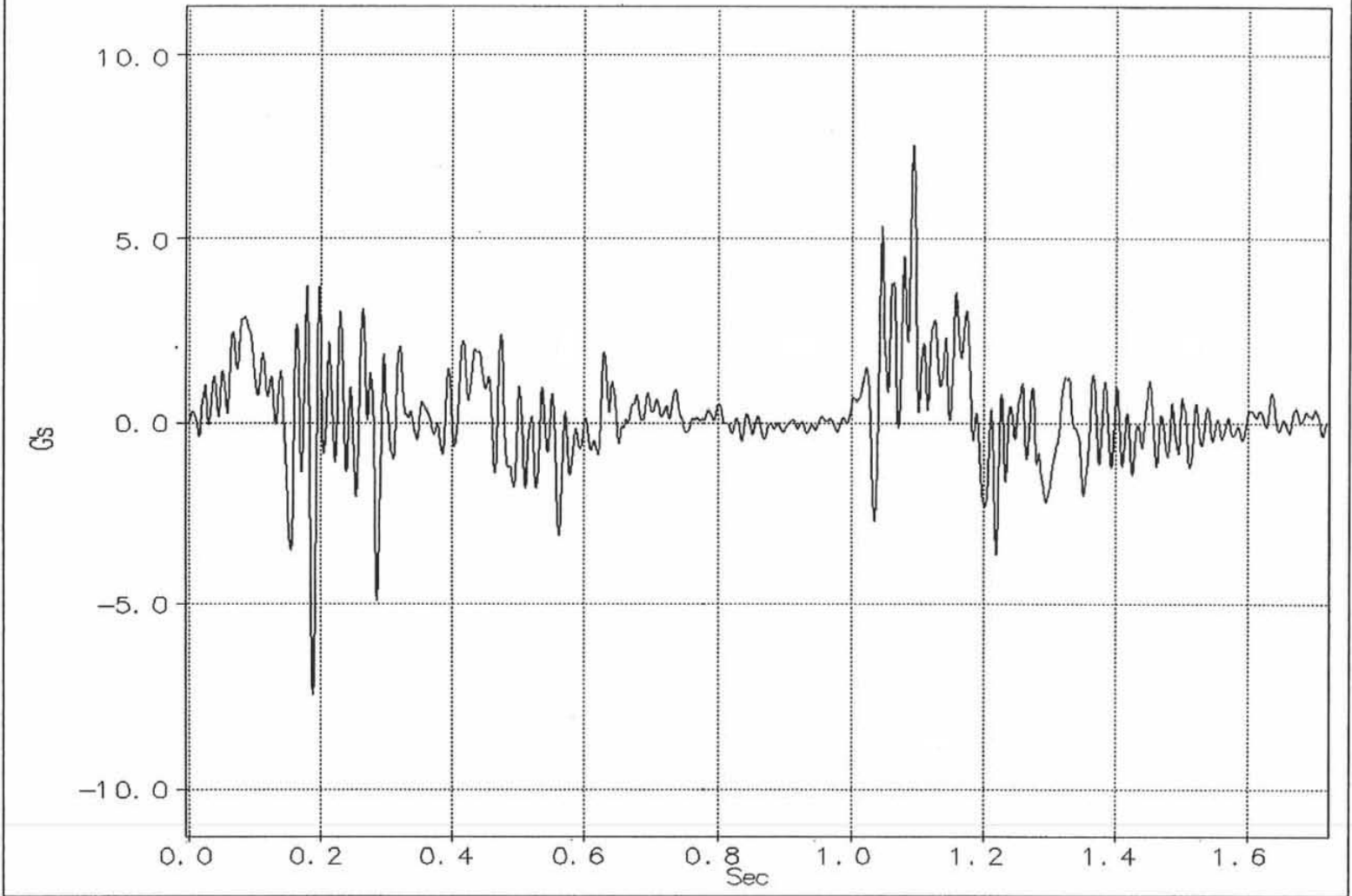


Figure A-3. Graph of Longitudinal Occupant Displacement, Test LVBR-1

LATERAL DECELERATION - TEST LVBR-1



75

Figure A-4. Graph of Lateral Deceleration, Test LVBR-1

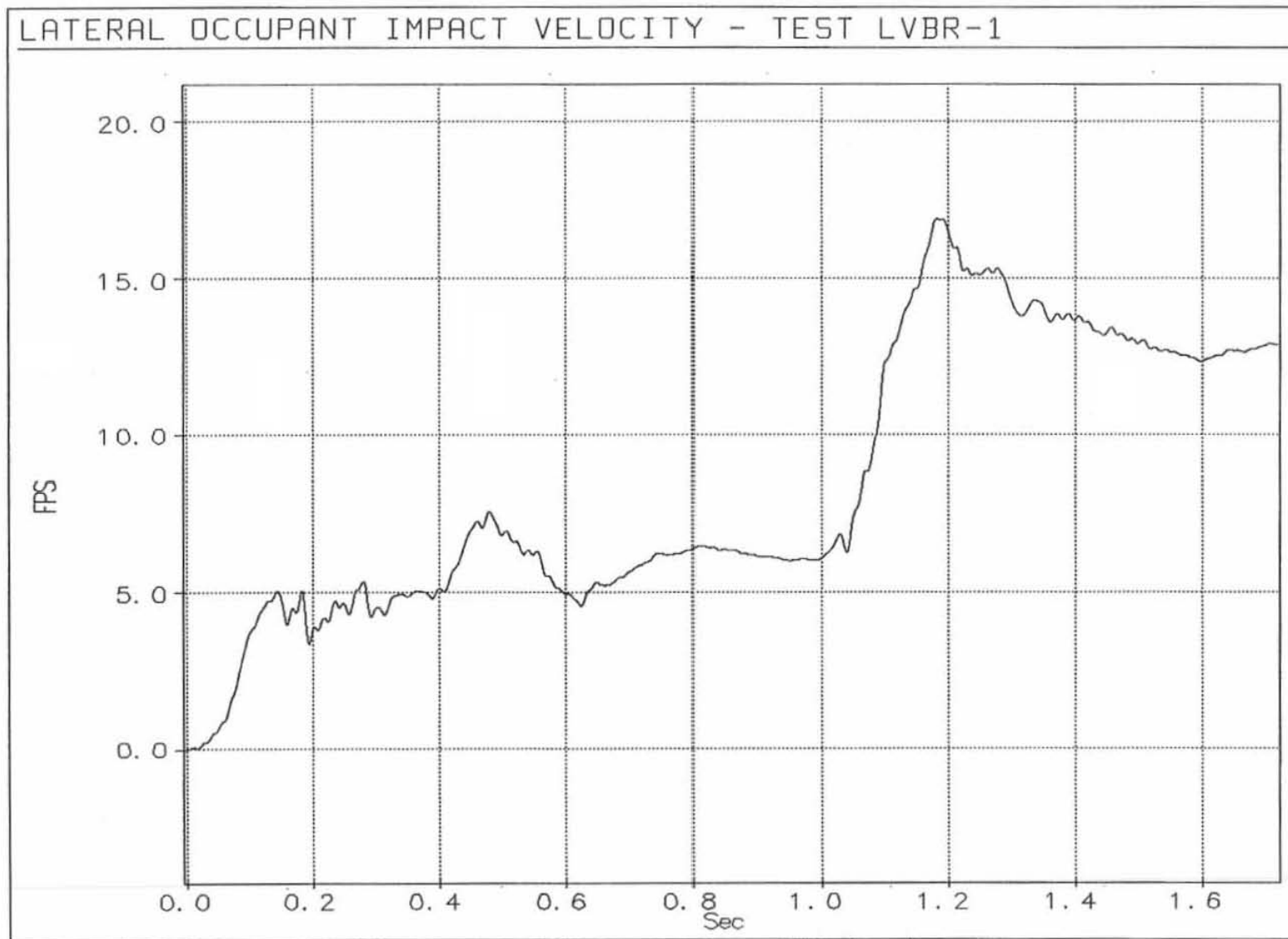


Figure A-5. Graph of Lateral Occupant Impact Velocity, Test LVBR-1

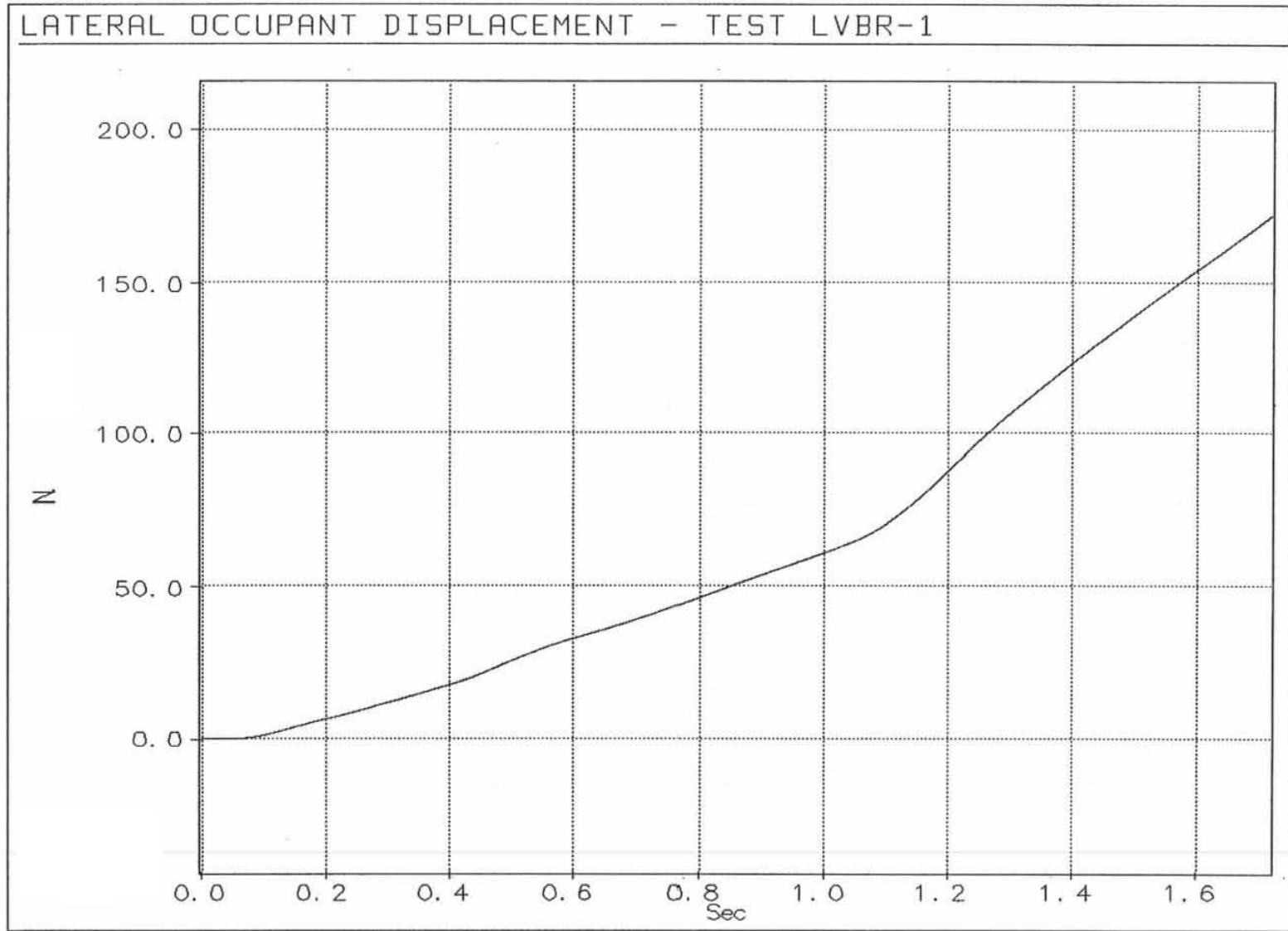


Figure A-6. Graph of Lateral Occupant Displacement, Test LVBR-1

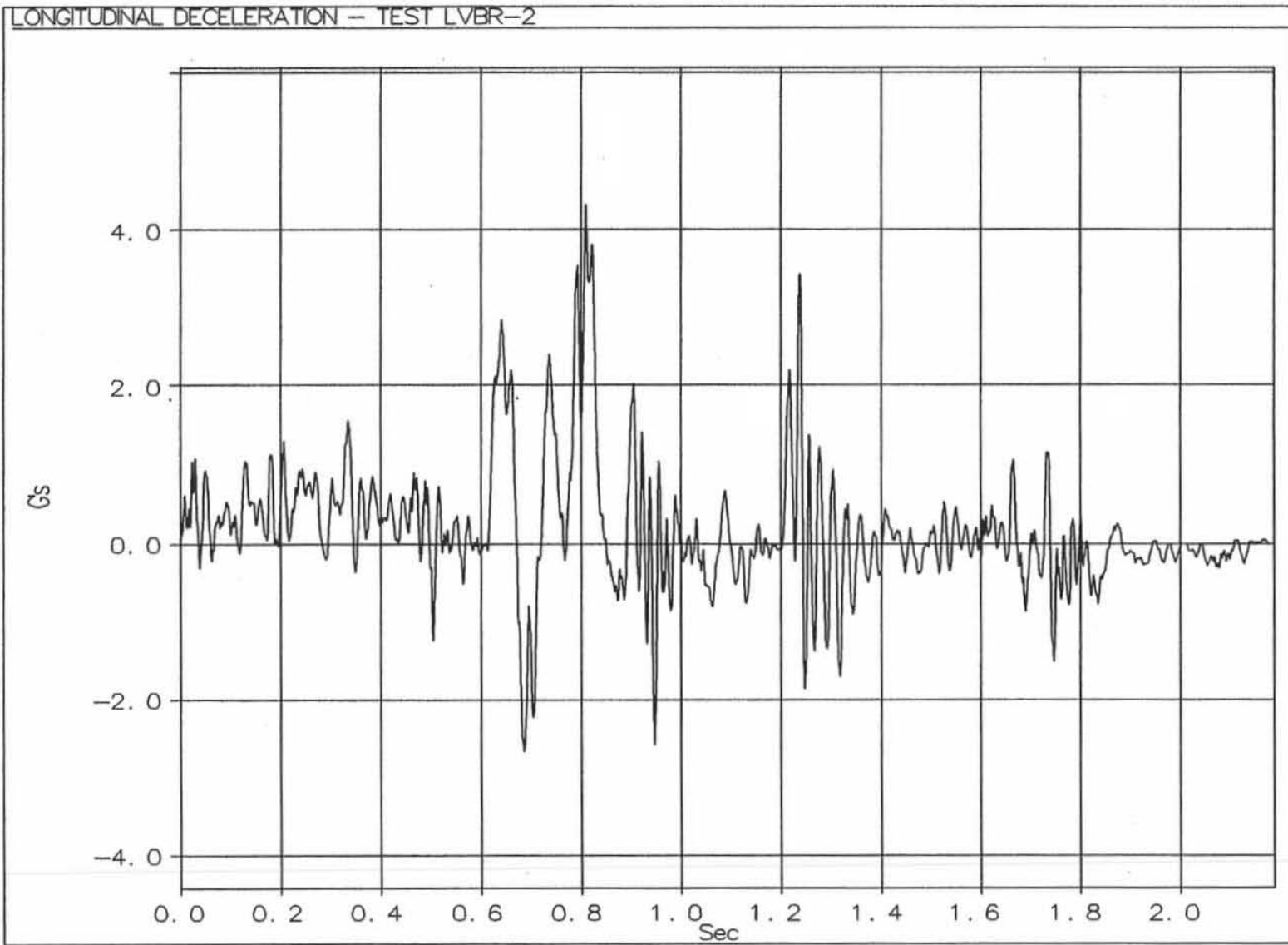


Figure A-7. Graph of Longitudinal Deceleration, Test LVBR-2

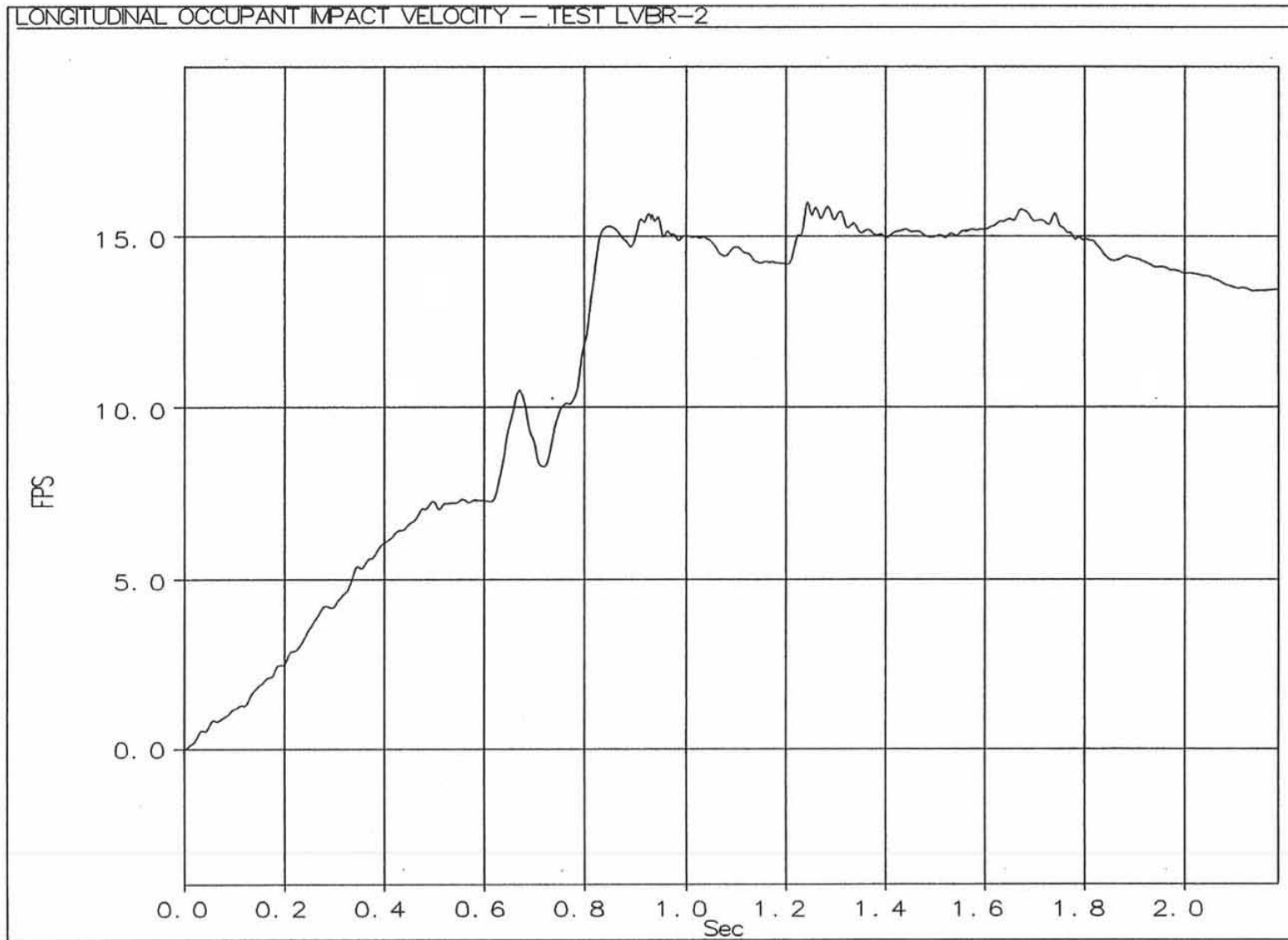


Figure A-8. Graph of Longitudinal Occupant Impact Velocity, Test LVBR-2

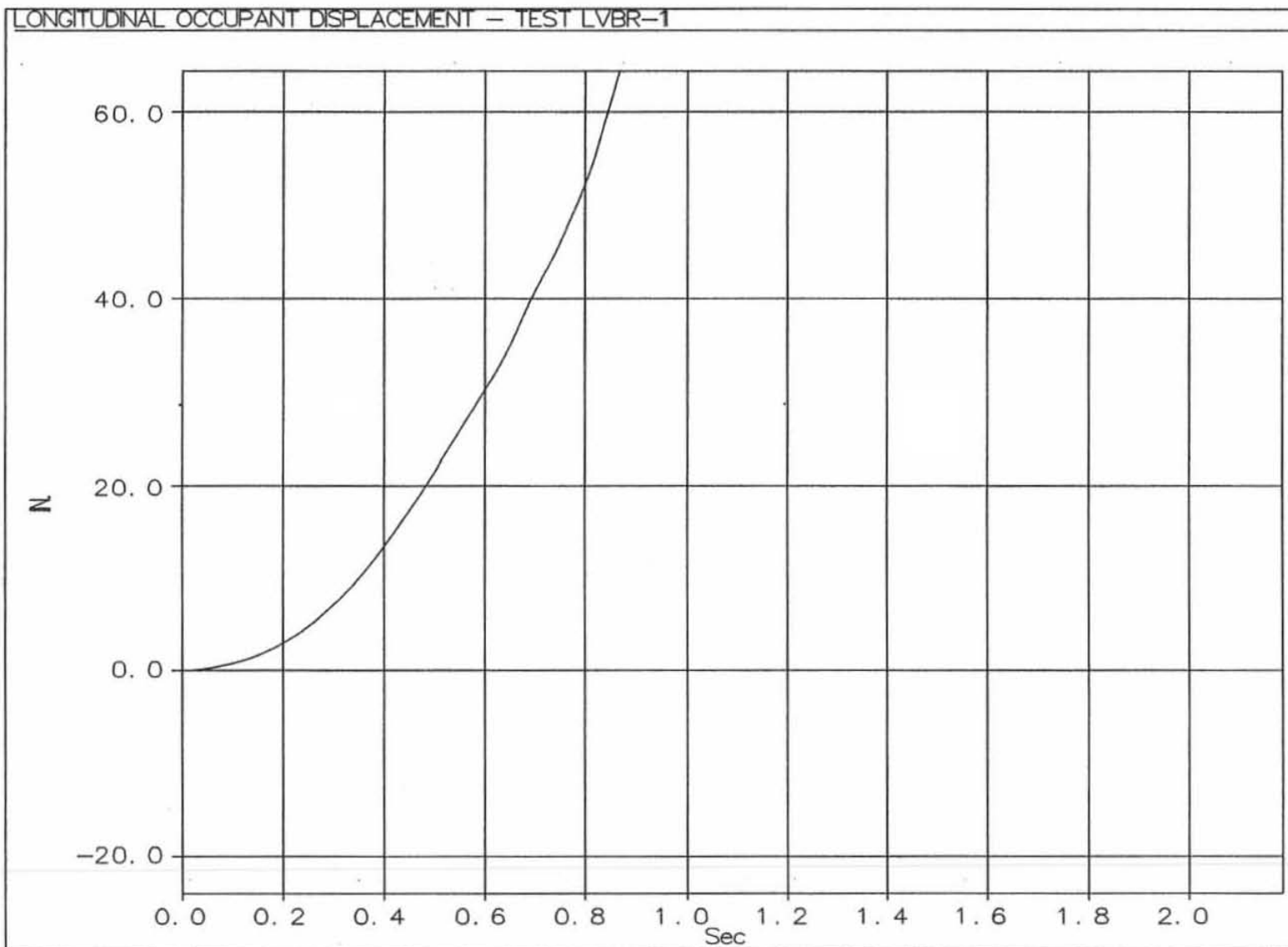


Figure A-9. Graph of Longitudinal Occupant Displacement, Test LVBR-2

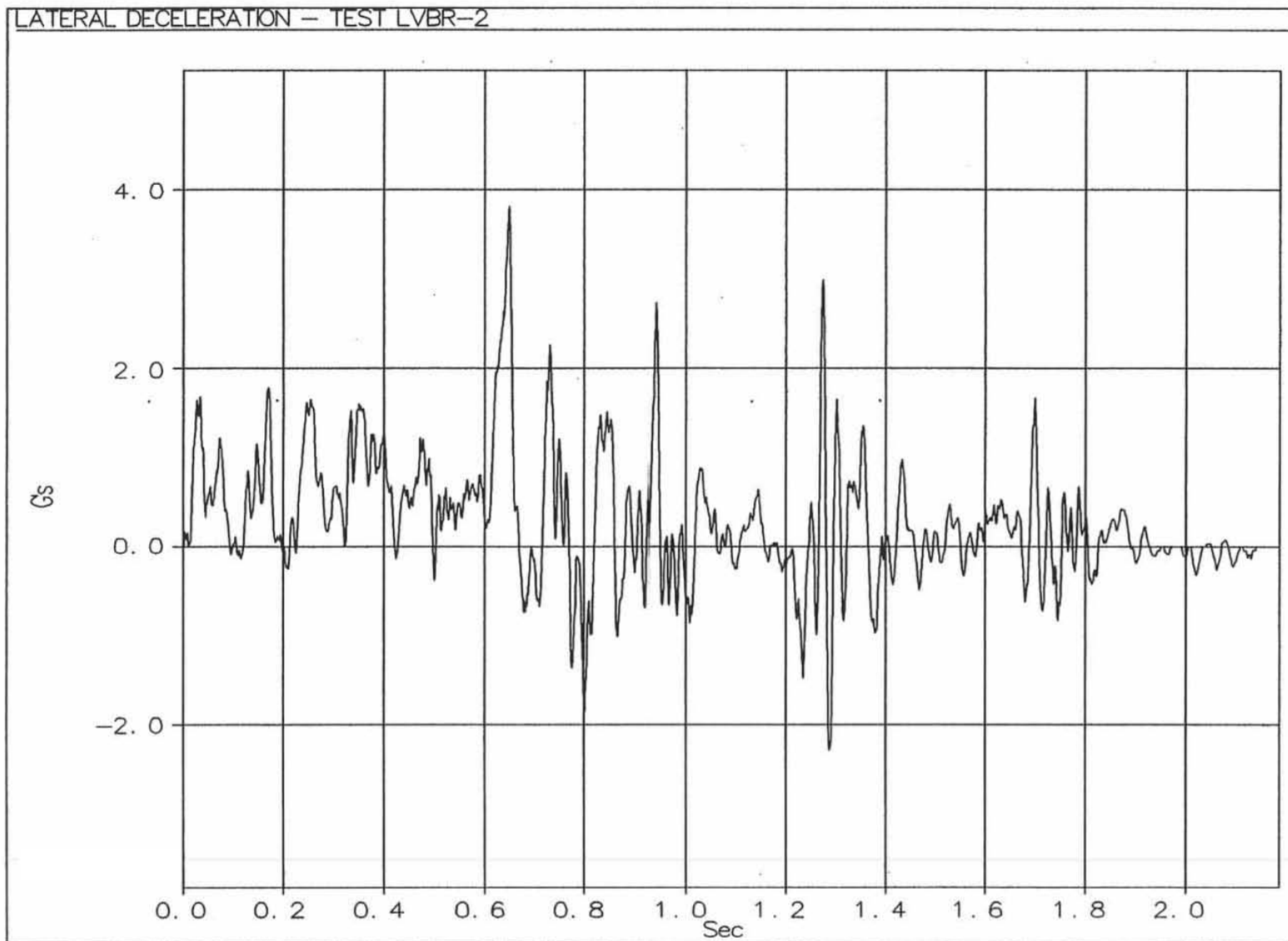


Figure A-10. Graph of Lateral Deceleration, Test LVBR-2

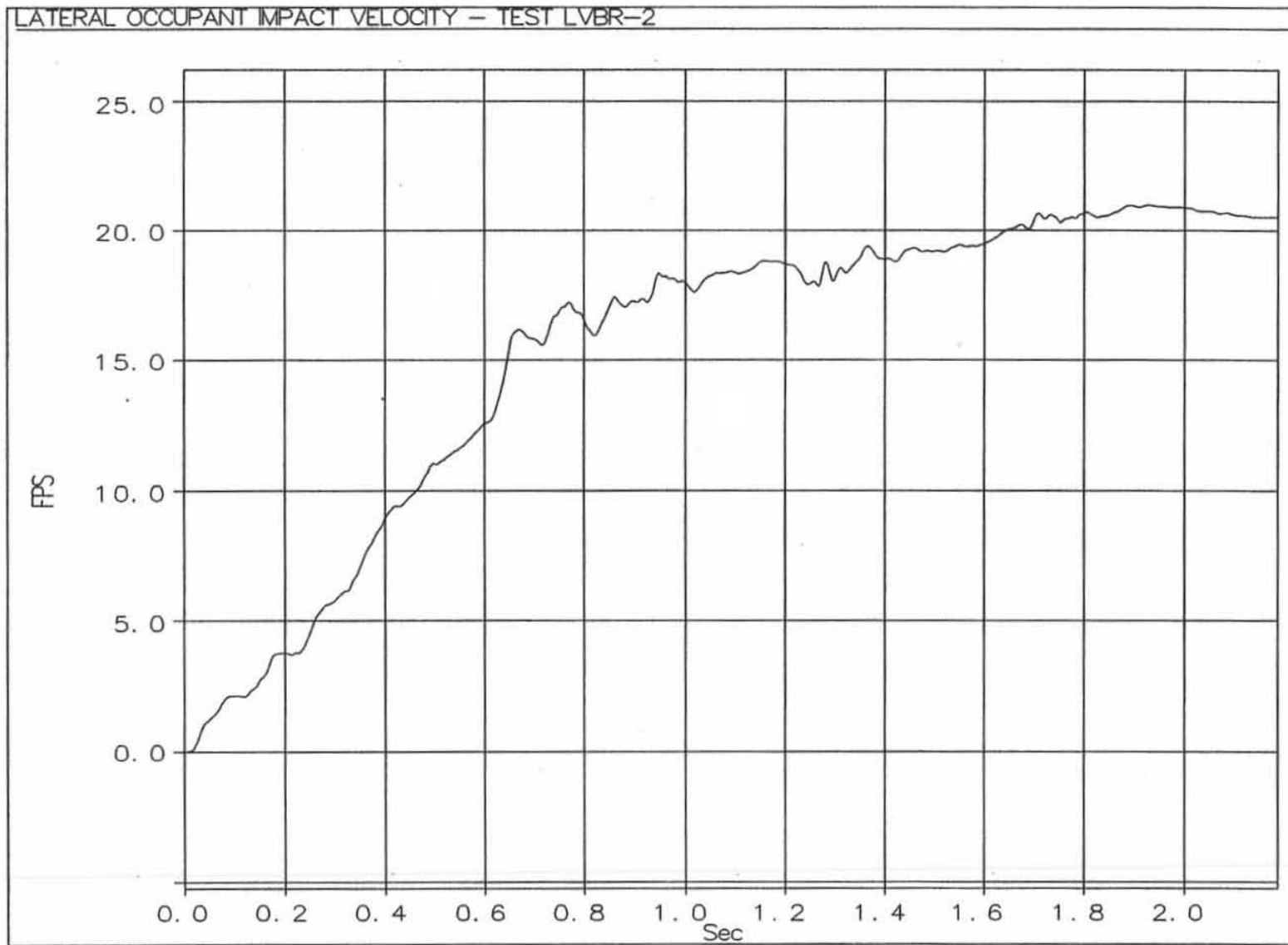


Figure A-11. Graph of Lateral Occupant Impact Velocity, Test LVBR-2

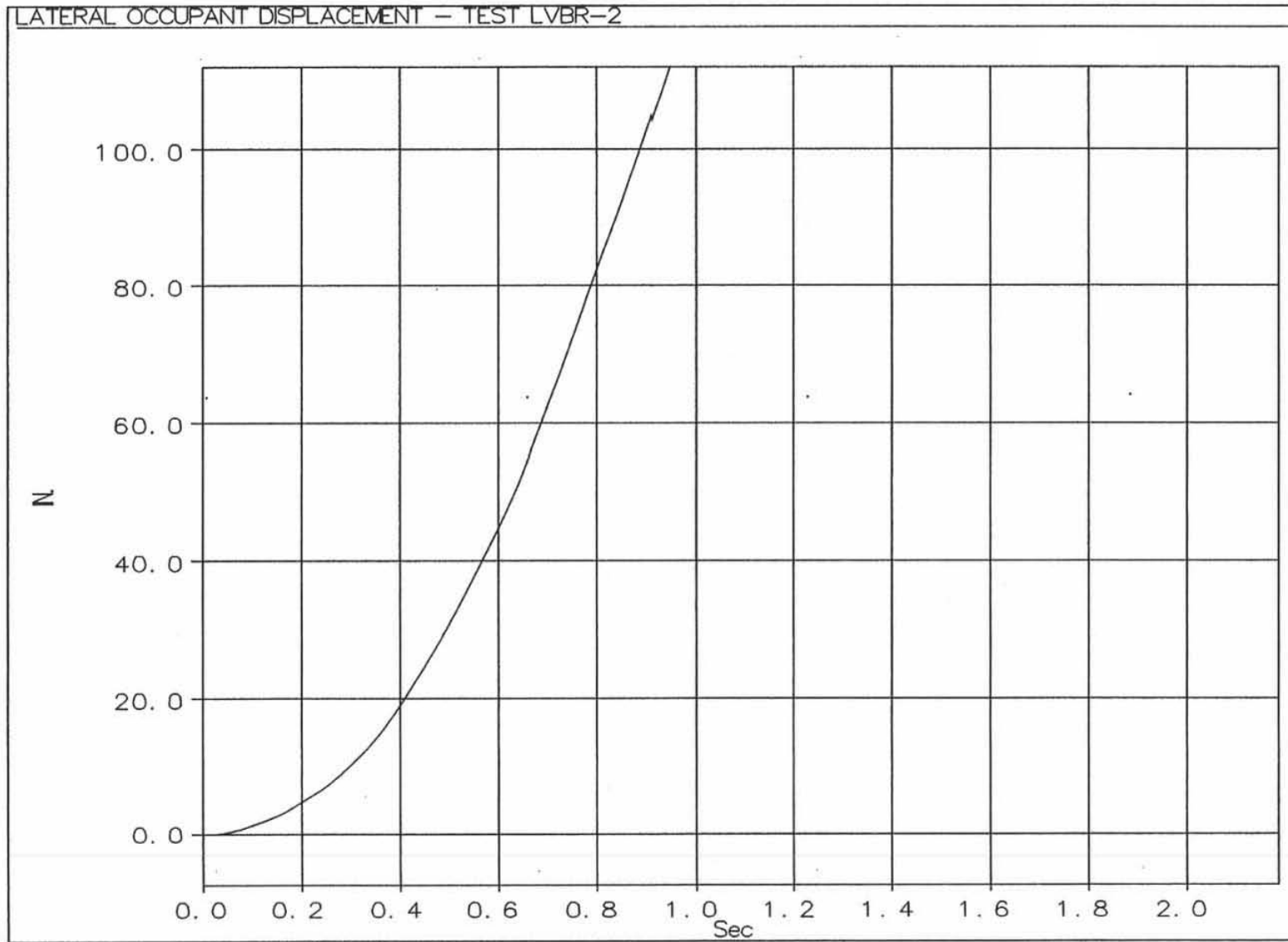


Figure A-12. Graph of Lateral Occupant Displacement, Test LVBR-2